Original Research Article

Plasmidome of an environmental *Acinetobacter lwoffii* strain originating from a former gold and arsenic mine

Tomasz Walter, Joanna Klim, Marcin Jurkowski, Jan Gawor, Iwona Köhling, Małgorzata Słodownik, Urszula Zielenkiewicz[*]

Institute of Biochemistry and Biophysics PAS, Pawiński ego 5a Str., 02-106 Warsaw, Poland

A B S T R A C T

Emerging important *Acinetobacter* strains commonly accommodate a plethora of mobile elements including plasmids of different size. Plasmids, apart from encoding modules enabling their self-replication and/or transmission, can carry a diverse number of genes, allowing the host cell to survive in an environment that would otherwise be lethal or restrictive for growth. The present study characterizes the plasmidome generated from an arsenic-resistant strain named ZS207, classified as *Acinetobacter lwoffii*. Sequencing effort revealed the presence of nine plasmids in the size between 4.3 and 38.4 kb as well as one 186.6 kb megaplasmid. All plasmids, except the megaplasmid, do apparently not confer distinguishing phenotypic features. In contrast, the megaplasmid carries arsenic and heavy metals resistance regions similar to those found in permafrost *A. lwoffii* strains. In-depth *in silico* analyses have shown a significant similarity between the regions from these plasmids, especially concerning multiple transposable elements, transfer and mobilization genes, and toxin-antitoxin systems.

Since *ars* genes encode proteins of major significance in terms of potential use in bioremediation, arsenic resistance level of ZS207 was determined and the functionality of selected *ars* genes was examined. Additionally, we checked the functionality of plasmid-encoded toxin-antitoxin systems and their impact on the formation of persister cells.

1. Introduction

Acinetobacter spp. are commonly isolated from various environments. Environmental strains are found in the soil, water and wastewater, where they can constitute up to 0.001% of the heterotrophic aerobic population (Kämpfer, 2014). In aquatic ecosystems, the most frequent habitat of *Acinetobacter* spp. is the surface layer of freshwater reservoirs and estuaries, in which fresh and seawater mix. Another place of *Acinetobacter* spp. occurrence is food, such as meat, vegetables, milk and dairy products.

The environment that deserves the most attention is the surface of the human body and the hospital environment. Skin spots that are characterized by high humidity, such as groin areas, armpits or spaces between the toes are a common source of *Acinetobacter* isolates (Dworkin et al., 2006). While *A. baumannii* is still by far the most common *Acinetobacter* species to cause infections (most of the clinical strains belong to *A. calcoaceticus - A. baumannii* complex), more of the lesser-known species, such as *A. ursingii*, *A. parvus* and most of all *A. lwoffii*, have been increasingly reported as hospital pathogens

associated with bacteremias (Turton et al., 2010). On the other hand, because of the ability to metabolize a variety of organic compounds *Acinetobacter* species, including *A. lwoffii,* are considered to have enormous biotechnological potential, especially in bioremediation. It is worth emphasizing that many of the compounds utilized by *Acinetobacter* spp. are toxic to most other organisms (Garrity and De Vos, 2005).

The metabolic abilities of *Acinetobacter* spp. that, in particular, characterize strains isolated from niches that require specific adaptations, like heavy metal-contaminated environments, are often attributed to their plasmids carrying genes that encode proteins allowing to degrade organic compounds (Dworkin et al., 2006). Also, genes connected with pathogenesis and responsible for antibiotic resistance are frequently located on plasmids. Since plasmids can be lost and acquired in response to changing environmental conditions, their ecological impacts are undisputed. In a given environment such additional genetic elements carry information that in given circumstances is beneficial for their host. Plasmid-encoded qualities include lots of profitable features that might be transferred *via* horizontal gene transfer. Therefore, it is

believed that plasmids play an essential role in evolutionary events of a given microbial community (Koonin and Wolf, 2008).

Since *A. lwoffii* is becoming more medically, but also ecologically relevant, many studies concerning environmental and clinical isolates have recently appeared (Das et al., 2016; Hu et al., 2011; Ku et al., 2000; Mittal et al., 2015; Turton et al., 2010). The emergence of strains which are able to colonize multiple environments and exchange genetic material by multiple methods is being noticed. This fact is tightly connected with the genetic properties of many environmental bacteria, including *Acinetobacter* spp., which are often characterized by an open pan-genome and high genetic plasticity (Imperi et al., 2011; Pagano et al., 2016; Poirel et al., 2011; Touchon et al., 2014). The acquisition of resistance determinants or features providing a selective advantage in particular niches is often the result of the transfer of mobile genetic elements like plasmids, insertion sequences (ISs), transposons or integrons (Peleg et al., 2008). Such transposable elements have the ability to move within the bacterial genome, which is considered one of the major causes of bacterial DNA rearrangements and changes in gene expression (Imperi et al., 2011; Lewin, 2004). Transposition events are observed both within the chromosome and plasmids, which themselves are the driving force for the evolution of bacterial species and cause an exchange of genetic material (Fondi et al., 2010).

In this work, we used a genomic approach to analyze the pool of plasmids of an environmental *Acinetobacter lwoffii* strain isolated from an arsenic-polluted environment and to identify genes potentially useful in bioremediation. The aim of this study was to assess the *A. lwoffii* ZS207 plasmidome content and basic properties of each plasmid, as well as special attention was paid to identify genes responsible for the ability of this strain to tolerate arsenic and several heavy metal compounds.

2. Materials and methods

2.1. Bacterial strains, plasmids and culture conditions

The bacterial strains and plasmids used in this study are listed in Table 1. The strains were typically grown in lysogeny broth (LB) medium (if required solidified by the addition of 2% (w/v) agar (LA)) at 37 °C (*Escherichia coli*) or 30 °C (*Acinetobacter lwoffii* ZS207). When necessary, the media were supplemented with antibiotics: ampicillin (100 μg/ml; recombinants carrying pGEM-T vector-based constructs) or chloramphenicol (10 μg/ml or 30 μg/ml; recombinants carrying pABB35 and its derivatives or recombinants carrying pACYC184 and its

derivatives). Species identification of strain ZS207 was conducted based on the 16S rRNA gene sequence as well as on the Average Nucleotide Identity (ANI) and DNA–DNA hybridization (DDH) values. The 16S rRNA gene was amplified using universal 27F/1492R primers (Table 2) and directly sequenced using the Sanger technique on an ABI3730 DNA Genetic Analyser (Applied Biosystems).

2.2. DNA manipulations and analyses

2.2.1. DNA extractions

The total genomic DNA of *A. lwoffii* ZS207 was isolated using CTAB/lysozyme method (Wilson, 2001) and DNA quality and quantity were checked on an agarose gel and fluorimetric measurements (Qubit 2.0, Life Technologies). Separately, isolation of plasmid DNA was carried out with the NucleoSpin Plasmid Midi Kit (Macherey-Nagel) following the manufacturer's instructions. Plasmid DNA concentration and purity were assessed with NanoDrop ND-1000 spectrophotometer (Thermo Scientific).

pGEM-T and pACYC184 plasmids derivatives were isolated from bacteria freshly cultured on LB (supplemented with proper antibiotic) using Gene Matrix Plasmid Miniprep Kit (EurX) and subsequently purified with Plasmid-Safe™ ATP-Dependent DNase (Epicentre).

pABB35 plasmid DNA was isolated from 1.5l bacterial culture (an overnight culture diluted 1/100 in fresh LB), supplemented with chloramphenicol and incubated at 37 °C with shaking until the exponential phase (OD_{600} 0.6–0.8). Then the culture was cooled on ice, centrifuged (9000 rpm, 10 min, 4 °C) and the cell pellet was processed with Nucleobond® AX PC100 kit (Macherey-Nagel) following the manufacturer's instructions.

2.2.2. Whole-genome shotgun sequencing and de novo assembly of the draft genome

The genome sequence was determined at the DNA Sequencing and Oligonucleotide Synthesis Laboratory of IBB PAS. Two sequencing technologies were used: Illumina and Oxford Nanopore MinION.

1.5 μg of the genomic DNA was sheared to an appropriate size by nebulization and used for paired-end library construction following the manufacturer's instructions (KAPA Biosystems) and sequenced using MiSeq instrument (Illumina). In addition, 1 μg of genomic DNA was used for Nextera Mate-Pair (Illumina) library preparation following the manufacturer's instructions and sequenced in paired-end mode (v3–600 cycle chemistry kit) on MiSeq instrument. In the next stage, long reads were generated for further bacterial genome assembly using

Table 1
Bacterial strains and plasmids used in this study.

Strain or plasmid	Characteristics	Reference or source
Acinetobacter lwoffii strain ZS207	environmental isolate	This study
Escherichia coli DH5α	F^- Φ80dlacZ recA1 endA1 gyrA96 thi-1 hsdR17 ($r_k^-m_k^+$) supE44 relA1 deoRΔ (lacZYA-argF)U196	(Hanahan, 1983)
pGEM-T-Easy	$oriV_{MB1}$, Ap^R, cloning vector	Promega
pABB35	$oriV_{RK2}$, Cm^R, unstable vector	(Bartosik et al., 2016)
pGEM-HigBA_pm	pGEM-T-Easy carrying HigBA1 operon from the pmZS; 745 bp fragment PCR-amplified using primers #1 and #2	This study
pGEM-HigBA_2	pGEM-T-Easy carrying HigBA2 operon from the pZS-2; 680 bp fragment PCR-amplified using primers #3 and #4	This study
pGEM-RelBE_2	pGEM-T-Easy carrying RelBE3 operon from the pZS-2, 671 bp fragment PCR-amplified using primers #5 and #6	This study
pGEM-YafQ/RelB_5	pGEM-T-Easy carrying YafQ/RelB operon from pZS-5; 804 bp fragment PCR-amplified using primers #7 and #8	This study
pGEM-YafQ/DinJ_4	pGEM-T-Easy carrying YafQ/DinJ operon from pZS-4; 973 bp fragment PCR-amplified using primers #9 and #10	This study
pGEM-RelBE_1	pGEM-T-Easy carrying RelBE operon from the pZS-1, 1118 bp fragment PCR-amplified using primers #11 and #12	This study
pGEM-BrnT	pGEM-T-Easy carrying BrnT toxin from the pZS-6, 754 bp fragment PCR-amplified using primers #13 and #14	This study
pABB35-HigBA_pm	pABB35 carrying HigBA_pm operon	This study
pABB35-HigBA_2	pABB35 carrying HigBA_2 operon	This study
pABB35-RelBE_2	pABB35 carrying RelBE_2 operon	This study
pABB35-YafQ/RelB_5	pABB35 carrying YafQ-RelB_5 operon	This study
pABB35-YafQ/DinJ_4	pABB35 carrying YafQ-DinJ_4 operon	This study
pABB35-RelBE_1	pABB35 carrying RelBE_1 operon	This study
pACYC184	$oriV_{p15A}$, Cm^R, Tc^R	Fermentas
pACYC184-arsC	pACYC184 carrying *arsC* gene from the pmZS	This study
pACYC184-arsBH	pACYC184 carrying *arsB* and *arsH* genes from the pmZS	This study

Table 2
Primers used in this study.

No.	Primer name	Targeted PCR product	Primer sequence (5′ → 3′)	Annealing temp. (°C)
1	Fhig_pm	HigBA_pm	GAGAAACGAGAGCTTACC	51.6
2	Rhig_pm		GGTACGACAGGAGTTATACC	
3	Fhig_2	HigBA_2	GCTTTAGGCGTGTTGTACTGTG	53.8
4	Rhig_2		GGCTGTTATACGAAATTAATGG	
5	Frel_2	RelBE_2	ACCAAAGTCTGAAAAATCCACCAA	54.7
6	Rrel_2		ATGGGAGCTATAAGCTCCCA	
7	Fyaf_5	YafQ/RelB_5	GAATTCTCAATGAAATACCCTCCCA	50.0
8	Ryaf_5		GCCCGACTTTGAAACATGGC	
9	Fyaf_4	YafQ/DinJ_4	CCAAATTAAGAGTTGTGCAAGA	49.7
10	Ryaf_4		AAACCATGTGTGCGTGTG	
11	Frel_1	RelBE_1	GAGATTTTAGGCTTATAGTG	45.0
12	Rrel_1		ATCTAAACTAATCGGTAGTG	
13	BrnT_F	BrnT	CTAAAATCGAGTATAGGCTGTAT	48.4
14	BrnT_R		ATCTTGAGAACTTAGCCAAGT	
15	27F_universal	16S rRNA gene	AGAGTTTGATCMTGGCTCAG	53.0
16	1492R_universal		TACGGYTACCTTGTTACGACTT	
17	arsC_F	ArsC	CGTGGATCCAATCTATACTCTAATATATGCTATTGCGAA	61.0
18	arsC_R		CCCAAGCTTCAACCATTATGTTAAATGAGGCGG	
19	arsBH_F2	ArsBH	CGTGGATCCCGTATAAGGTGTATGATGTTAATTTTAGG	67.5
20	arsBH_R2		CCCAAGCTTTTTCATAAGGTGTGTTCAGCGGA	

the MinION nanopore sequencing instrument (Oxford Nanopore Technologies, Oxford, UK). Approximately 1 µg of bacterial HMW (high-molecular-weight) DNA was used for the library preparation. Long nanopore reads were assembled in a hybrid mode with Illumina data using Unicycler v.0.4.7 (Wick et al., 2017). The remaining sequence errors in the genome assembly were verified by the PCR amplification of DNA fragments, followed by Sanger sequencing. All of the sequence errors and misassemblies were further corrected using Seqman software (DNAStar, USA) to obtain the complete nucleotide sequence of the bacterial genome.

The genome sequence was annotated with the Prokka (Seemann, 2014), which is the Prodigal-based pipeline. Prokka incorporates a number of other feature-specific tools: HMMER, Aragorn, Infernal, Barrnaap, minced, RNAmmer, SignalP; for details and references refer to Prokka pipeline description (http://www.vicbioinformatics.com/software.prokka.shtml). The annotations of the plasmids pZS1–9 and metal resistance genes located on the megaplasmid were verified with RAST annotation server (Aziz et al., 2008; Overbeek et al., 2014), Patric annotation pipeline (Wattam et al., 2017) and BLAST (Altschul et al., 1990) results and manually corrected.

The complete chromosome and plasmid sequences of ZS207 strain were deposited at GenBank (NCBI) under the project accession number: BioProject: PRJNA359405.

2.2.3. Taxonomic assignment

Average Nucleotide Identity (ANI) between ZS207 chromosome and closely related genomes was calculated using Kostas Lab ANI calculator (Rodriguez-R and Konstantinidis, 2014) and OrthoANIu (Yoon et al., 2017). *In silico* DNA-DNA hybridization (DDH) was performed using Type (Strain) Genome Server (TYGS) (Meier-Kolthoff and Göker, 2019).

To calculate genome distances and generate the tree, the Type (Strain) Genome Server (TYGS) was used; for methodology details refer to the server methods description. In brief, the tree was inferred with FastME 2.1.6.1 from the Genome BLAST Distance Phylogeny (GBDP) distances calculated from genome sequences. The branch lengths are scaled in terms of GBDP distance formula d5. The numbers above branches are GBDP pseudo-bootstrap support values > 60% from 100 replications, with an average branch support of 53.5%. The tree was rooted at the midpoint.

2.2.4. XerC/D recognition sites identification

ZS207 strain plasmid nucleotide sequences were queried using Fuzznuc (http://www.bioinformatics.nl/cgi-bin/emboss/fuzznuc) with

an ambiguous XerC/D nucleotide recognition sequence (NNTNYKYA-TAANNNNYWTTATSTKAWNN, where Y = C/T, K = G/T, W = A/T, S = G/C, N = A/T/C/G), inferred from the consensus 28-mer XerC/D recognition sequence determined for *A. baumannii* plasmids (Cameranesi et al., 2018).

2.2.5. TA genes identification

Toxin-Antitoxin (TA) systems genes were identified primarily using the TAfinder, an online TA loci prediction tool (http://202.120.12.133/TAfinder/index.php; Xie et al., 2018). The completion of the list of toxins and antitoxins was done based on the results of the annotation process. All TA genes were verified manually *via* comparison of its translated nucleotide sequences with NCBI refseq_protein and Uni-ProtKB databases.

2.2.6. Replication genes identification and classification

The identification of plasmid replication genes was done based on the results of the annotation process followed by manual verification. In addition, *in silico* PCR-based replicon typing (PBRT) with primers developed for the purpose of *A. baumannii* plasmid typing (Bertini et al., 2010) was performed. Furthermore, primers designed for *A. baumannii* MLST were tested *in silico* and also a replicon identification with PlasmidFinder was performed (Carattoli et al., 2014).

Rep_3 database sequences used for the calculation of the phylogenetic tree and replication genes classification were used according to (Salto et al., 2018). Protein alignments were carried out using ClustalOmega (Madeira, 2019) default parameters. Rep_3 family phylogenetic analysis was carried out by maximum likelihood (ML) using PhyML 3.0 (Guindon et al., 2010). The best evolutionary model for each multiple alignment was established by ProtTets 3.4.2 (Darriba et al., 2011). Bootstrap values of 100 were chosen for ML analysis. The phylogenetic tree was generated using iTOL v5.5 (Letunic and Bork, 2019).

2.2.7. Prophage regions identification

The prophage sequences were identified using PHASTER, a web server for prophage identification and annotation (Arndt et al., 2016). Nucleotide sequences of all ZS207 strain replicons were used as input.

2.2.8. Plasmids sequences comparisons

Visualizations of plasmid sequences comparisons were conducted with Circoletto visualization tool (Darzentas, 2010). Nucleotide sequences of *A. lwoffii* ZS207 strain plasmids were used as the query for the comparisons. To compare plasmids of the ZS207 strain with each

other, the database consisted of the tested strain plasmids sequences, whereas for the comparison with other *A. lwoffii* plasmids, the database was created from the sequences of all *A. lwoffii* complete plasmid sequences available in the nucleotide NCBI reference sequences database at that time; only the sequences that produced hits were shown. Default Circoletto parameters were used, except using % identity to colour the ribbons, absolute score/ribbon colouring with custom % of identity thresholds for each colour and switching off orientation lights. Following Circoletto guidelines, the *E*-value for blastn alignment was changed to 1e-40 (1e-10 is the default) when comparing with other *A. lwoffii* plasmid sequences to ensure clarity. The Circoletto algorithm also automatically reduces the number of visible similarities (ribbons) to ensure the clarity of the rendered image.

2.3. Construction of pABB35 derivatives for determination of the TA system's functionality

Six potential complete TA systems and one unaccompanied toxin were chosen for the analysis. Primers used to amplify potential TA genes were designed based on *A. lwoffii* ZS207 draft genome sequence (custom sequenced and assembled) and are listed in Table 2.

PCRs were performed using the OptiTaq DNA Polymerase (EurX) with appropriate primer pairs (Table 2) and genomic DNA of *A. lwoffii* ZS207 at concentration 10 ng/µl as a template. The following thermocycle was applied using a Labcycler (SensoQuest) to amplify the desired products: initial denaturation at 95 °C for 2 min followed by 26 cycles of denaturation at 95 °C for 20 s, annealing (at temperature depending on the primer pair) for 30 s, extension at 72 °C for 1 min/kb, and a final extension at 72 °C for 7 min.

Amplified fragments were separated by 0.9% agarose gel electrophoresis. PCR products were purified with NucleoSpin® Gel and PCR Clean-Up (Macherey-Nagel) and ligated with pGEM-T cloning vector (pGEM®-T Vector System) according to the manufacturer's protocol (Promega). Ligation products were transferred to *E. coli* DH5α cells *via* electroporation and transformants were selected on LA plates supplemented with ampicillin (100 µg/ml), IPTG and X-gal, incubated overnight at 37 °C.

Potential transformants carrying desired recombinant plasmids were transferred to LB medium supplemented with ampicillin and were grown overnight at 37 °C. pGEM-T plasmid derivatives were isolated from bacterial cultures using Gene Matrix Plasmid Miniprep Kit (EurX). The presence of the insert in plasmid derivatives was confirmed by PCR and restriction enzyme digestion. The sequence of each cloned fragment was verified by Sanger sequencing.

Subsequently, pGEM-T-based plasmid constructs were digested with *Sac*I and *Nco*I FastDigest™ restriction enzymes according to manufacturer's conditions (Thermo Scientific). The products of the reaction were separated on a 0.9% agarose gel and followed by insert excision and purification (NucleoSpin® Gel and PCR Clean-Up, Macherey-Nagel).

In parallel, the pABB35 vector was also digested with SacI and NcoI and then ligated using T4 ligase with each of the purified inserts (containing TA cassette). Subsequently, electrocompetent *E. coli* DH5α cells were transformed with a ligation mixture, plated onto LA medium supplemented with chloramphenicol and incubated overnight at 37 °C. The presence of TA cassettes in pABB35 derivatives was confirmed by PCR.

2.4. Plasmid stability assay

Cultures of *E. coli* DH5α carrying pABB35 vector or its derivatives were grown overnight in LB medium containing selective antibiotic (chloramphenicol) at 37 °C. Overnight bacterial cultures were diluted to $OD_{600} = 0.05$ in fresh LB medium without an antibiotic and were grown with shaking for up to 16 (or 30 - see Supplements) generations. To analyze plasmid retention aliquots of appropriate cultures, dilutions prepared at the beginning of the experiment and every 3 h were plated onto antibiotic-free LA plates to get approximately 100–200 colonies, and then 100 colonies were re-streaked onto LA plates with a selective antibiotic. Plasmid retention was expressed as the percentage of Cm^R colonies.

2.5. Persistence assay

The determination of *A. lwoffii* ZS207 persistence cells frequency was measured comparing CFUs in cultures exposed to different types of stress with those not exposed to stress. The following experimental protocol (in which elements from (Dörr et al., 2010; Maisonneuve et al., 2011) were included) was used: overnight cultures were 100-fold diluted in fresh media and incubated with shaking until OD_{600} reached 0.2. An appropriate dose of a stress factor (650 mM NaCl or 60 °C) was applied for 20 min and culture's aliquots were plated on LA (after the samples were spun down, washed and resuspended in 0.9% NaCl). Then, the cultures were subjected to a lethal dose of a given antibiotic and further incubated for 4 h. After that, aliquots of cultures were sampled, washed to remove antibiotic as described above, properly diluted and plated onto LA. Persisters were calculated each time by dividing the number of CFU/ml in the stressed culture by the number of CFU/ml in the culture without application of the stress factor. The following antibiotics were applied: ampicillin 100 µg/ml and streptomycin 100 µg/ml. Cell growth was determined by monitoring the OD_{600}. In parallel, the same cultures not exposed to stress were cultivated and their CFUs were determined.

2.6. Heavy metal and arsenic Salts' resistance tests

Overnight bacterial cultures were 100-fold diluted in fresh LB or M9 (with 0.1% casamino acid and 0.4% glucose) medium supplemented with heavy metals or arsenic salts. The salts used in the resistance assay and their concentrations (mM) tested were as follows: $K_2Cr_2O_7$: 0.3, 0.6, 0.9, 1.2, 1.5 and 1.8; $CoSO_4 x7H_2O$: 0.01, 0.05, 0.1, 0.2, 0.3, 0.5 and 1.0; $ZnCl_2$: 0.2, 0.4, 0.8, 1, 1.2, 1.4, 1.6, 3.2 and 6.4; $HgCl_2$: 0.015, 0.03, 0.06; $Ni(NO_3)_2$: 0.45, 0.9, 1.8, 2.7; $CuSO_4$: 0.9, 1.8, 2, 2.2, 2.4, 2.7, 3.6, 4.0; $CdCl_2$: 0.01, 0.025, 0.05, 0.07, 0.1, 0.12, 0.14, 0.16, 0.18, 0.2, 0.3, 0.4; $NaAsO_2$ [As(III)]: 5, 6, 7, 10, 15, 20, 25, 30, and 60; $Na_2HAsO_4 x7H_2O$ [As(V)]: 10, 30, 60, 100, 150, 200, 220, 250, 300, 500, 650, 750, 800, 950 and 1000. Then the cultures were incubated with shaking for 48–72 h at 28/30 °C (*A. lwoffii* ZS207) or 37 °C (*E. coli* DH5α) and visually inspected. An increase in optical density (OD_{600} spectrophotometer measurements) in the presence of the aforementioned heavy metal and arsenic ion concentrations were considered as resistance.

2.7. Antibiotic susceptibility/resistance test

Antibiotic susceptibility of the *A. lwoffii* ZS207 was determined by the disk diffusion assay. Bacteria were cultured at 30 °C to $OD_{600} = 0.6$ and 400 µl aliquots were plated onto AM3 (Antibiotic Medium 3, Oxoid) plates. Filter-paper disks were then placed on the surface of the agar medium and impregnated with 2.5 µl of each tested antibiotic. The following antibiotics were used: ampicillin, chloramphenicol, erythromycin, gentamicin, kanamycin, nalidixic acid, neomycin, pefloxacin, piperacillin, rifampicin, spectinomycin, streptomycin, telithromycin and tetracycline, each at a concentration range between 0.5 and 300 µg/ml. The AM3 agar plates containing the bacteria inoculum and antibiotics disks were further incubated at 30 °C for 24 h. Antibiotic susceptibility was determined by measuring the diameter of the zones of bacterial growth inhibition around the antibiotic disks.

2.8. Construction of pACYC184 derivatives for determination of selected ars genes functionality

The *arsC* and *arsB* genes were selected for the analysis. Primers used to amplify the *ars* genes were designed based on *A. lwoffii* ZS207 draft genome sequence (custom sequenced and assembled) and are listed in Table 2.

PCRs were performed using the Phusion Green Hot Start II High-Fidelity (Thermo Scientific) with appropriate primer pairs (Table 2) and genomic DNA of *A. lwoffii* ZS207 at concentration 10 ng/µl as a template. The following thermocycle was applied using a Labcycler (SensoQuest) to amplify the desired products: initial denaturation at 98 °C for 30 s followed by 26 cycles of denaturation at 98 °C for 10 s, annealing (at temperature depending on the primer pair) for 30 s, extension at 72 °C for 30 s/kb, and a final extension at 72 °C for 7 min.

The amplified fragments were purified with NucleoSpin® Gel and PCR Clean-Up (Macherey-Nagel). Then, PCR products and the vector pACYC184 were digested with *Hin*dIII and BamHI FastDigest™ restriction enzymes according to the manufacturer's conditions (Thermo Scientific). Subsequently, the products of the reaction were separated on a 0.9% agarose gel followed by purification (NucleoSpin® Gel and PCR Clean-Up, Macherey-Nagel) and ligated using T4 ligase. Then, chemocompetent *E. coli* DH5α cells were transformed with a ligation mixture, plated onto LA medium supplemented with chloramphenicol and incubated overnight at 37 °C. The presence of desired recombinant plasmids in transformants was confirmed by PCR and then the sequence of both cloned fragment was verified by Sanger sequencing.

3. Results and discussion

The studied strain ZS207 was isolated in 2012 from a beaker in which arsenical waste culture media were being temporarily stored as an outgrowing bacterium. These media were used for culturing newly isolated strains from a biofilm developing on the rock walls in the ancient Złoty Stok gold and arsenic mine in order to investigate their arsenic resistance. Both, arsenate and arsenite ions were present in the wastes in high amounts. After obtaining a pure culture, the strain was checked for the ability to grow in the presence of arsenic showing resistance up to 750 mM of arsenate and 30 mM of arsenite ions. This unique feature prompted us to study the isolated strain more deeply.

3.1. General characteristics of the A. lwoffii ZS207 strain

The 16S rRNA gene sequence of the ZS207 strain, 1433 nt in length, was an indication that the taxonomic position of the strain is in the *Acinetobacter* genus. The sequence clustered tightly with 16S rRNA sequences of type strains of *A. lwoffii* and *A. pseudolwoffii*.

The results of calculated Average Nucleotide Identity (ANI) between ZS207 chromosome and closely related genomes confirmed the results of 16S rRNA genes analysis. *A. lwoffii* NCTC 5866 was the only analyzed *Acinetobacter* species type strains with ANI value above the threshold for the same species classification (Kostas Lab ANI calculator value 96.16%; OrthoANIu value 96.24%), which is above 95% or 96% according to Goris et al., 2007 and Colston et al., 2014, respectively. The results of DDH analysis were consistent with 16S rRNA genes analysis and ANI calculation. The DDH value above 70% is considered a threshold for the same species classification and the only analyzed *Acinetobacter* species type strains with DDH value above the threshold was *A. lwoffii* NCTC 5866 with DDH value 77.4%. *In silico* DDH results were also used to construct a phylogenetic tree (Fig. 1).

Despite a growing interest in the *Acinetobacter* genus, none of the *A. lwoffii* genome sequences deposited at the time of the ZS207 strain identification was completed and annotated. What is more, only one paper concerning a detailed plasmidome analysis of environmental *A. lwoffii* strains (all of them were isolated from permafrost sediments) has been recently published (Mindlin et al., 2016).

A. lwoffii ZS207 forms colonies that are smooth and circular in form. They lack pigmentation and are half-translucent. The tested strain grows in an undisturbed way up to 39 °C with an optimal temperature around 30 °C; nonetheless, it can survive up to 65 °C. The bacteria could not grow at a relatively acidic and basic pH - the strain was found to grow between the pH levels of 6.0–9.5 with pH of 7.0–7.5 as an optimum. Maximum salt concentration tolerated by the isolate is 5%, while the optimal concentration is between 1.4 and 1.8%. At higher salinities (up to 5%) its growth is perceptible but strongly reduced. The tested ZS207 isolate is resistant to a number of antibiotics: chloramphenicol, erythromycin, kanamycin and spectinomycin and is susceptible to nalidixic acid, pefloxacin, gentamicin, rifampicin, telithromycin, neomycin, piperacillin, tetracycline, streptomycin and ampicillin.

3.2. Extrachromosomal DNA elements from the strain ZS207

Preliminary analyses with the use of different extraction and electrophoretic techniques suggested the presence of eight plasmids of disparate sizes and one megaplasmid of about 200 kb in this strain. To confirm these findings and gain insight into the plasmid content an exhaustive sequencing of the whole genome of ZS207 strain was performed. The combined data gathered from the Illumina MiSeq and Oxford Nanopore MinION sequencing technologies resulted in a high-quality hybrid genome assembly, which revealed one circular chromosome of 3,259,224 bp, nine complete circular plasmids in the size of 4.3–38.4 kb and one megaplasmid (186.6 kb). In this work, we focus on the extrachromosomal elements present in *A. lwoffii* ZS207.

3.2.1. Plasmid content

The members of the *Acinetobacter* genus commonly contain multiple plasmids (Lean and Yeo, 2017; Mindlin et al., 2016), so the existence of 10 extrachromosomal elements in the studied strain is not extraordinary. However, the knowledge of ZS207 plasmids sequences, their coding potential and the mechanisms allowing their coexistence are a value in general plasmid biology. Also, it is worth mentioning that there are merely 41 sequences of complete and annotated *A. lwoffii* plasmids in the NCBI database. The comparison of plasmid sequences within the ZS207 strain plasmidome as well as with other *A. lwoffii* plasmids is the subject of Section 3.2.5. The GC content of ZS207 megaplasmid is 40.3% and for other plasmids it varies from 34.4% to 37.9%, whereas it is 43.2% for the chromosome sequence. This parameter is similar to other *A. lwoffii* plasmids that can presently be found in the NCBI database, in which the calculated mean GC content is 39.3% and is generally higher in mega-sized plasmids. To fully exploit the coding potential of plasmid sequences, we compared annotation data from 4 sources, namely Prokka, RAST, Patric and NCBI reference protein database. Good practice in plasmid annotation suggested by Thomas and coauthors (Thomas et al., 2017) was followed to describe plasmid content.

A deeper insight into the plasmids content revealed the presence of 342 protein-coding genes in total, 206 of them located on the megaplasmid. Currently, the function of just over half of the ORFs still remains unknown. The proportion of hypothetical protein CDSs is similar to the results of plasmid annotation in environmental *Acinetobacter* strains (Salto et al., 2018). At the same time in plasmids from clinical isolates only 4% of genes were reported to encode hypothetical proteins by these authors. It could be hypothesised that environmental plasmids are understudied and hence many of their genes encode proteins with so far unidentified functions. All predicted genes of ZS207 plasmids are listed in Table S1.

The overall structure, gene content and characteristics of ZS207 strain plasmids are presented in Fig. 2 and Table 3. For clarity, the comparison between the content of the pmZS megaplasmid and other plasmids is presented separately in Fig. S1. The comparison of plasmid sequences within the ZS207 strain revealed that there are numerous
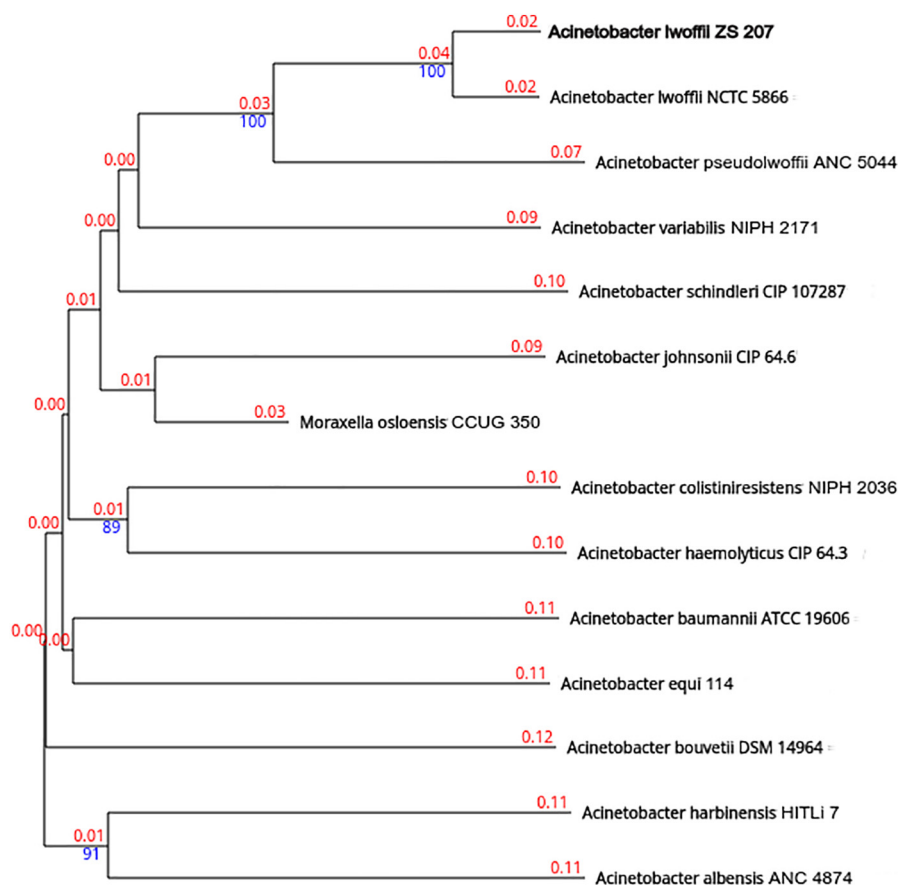
Fig. 1. Phylogenetic tree showing the position of the *A. lwoffii* ZS207 strain relative to type strains of *Acinetobacter* species based on the *in silico* DDH results. The *Moraxella osloensis* sequence was used as an outgroup. To calculate genome distances and generate the tree, the Type (Strain) Genome Server (TYGS) was used.

regions of significant similarity across the smaller plasmids, which include mostly replication, mobilization and TA systems genes, as well as a number of transposable elements genes, which is also a feature of the megaplasmid (as shown in Fig. 2 and Fig. S1). Most of them occur between the megaplasmid and the pZS-1 and pZS-2 plasmids, which is consistent with the presence of similar transposase and insertion sequence genes within those replicons. This may indicate that bigger plasmids are mosaic structures comprised of fragments of different origins. The region, which is present in two very similar copies within the megaplasmid, is comprised of several hypothetical protein genes flanked by transposase genes. Thus, it is probably a transposable mobile genetic element. The only plasmid with no region of high similarity to other ZS207 plasmids is pZS-8. The distinctive presence of many of the above-mentioned TA systems is the subject of the detailed analyses described in Section 3.4. No antibiotic or other stress resistance determinants were found in the plasmid sequences, except in the megaplasmid. The lack of knowledge about predicted genes function hinders a more precise description of the structure of plasmids; for example, whether they are modular or not.

Plasmids pZS-1, -2 and -3 contain a number of hypothetical protein genes. Among these three plasmids, the highest number of hypothetical ORFs occurs in pZS-1 and it constitutes 68% of total ORFs and 60% of the plasmid sequence. Apart from hypothetical protein genes, several transposases and ISs genes were found in these three plasmid sequences as well as individual genes of defined function were identified, including two transferases. Also, four phage-derived genes were found in the pZS-1 plasmid.

The six smallest plasmids contain predominantly genes related to replication, conjugal transfer and mobilization. The predicted conjugal transfer protein is TraD and its gene sequences from plasmids pZS-4, -7

and -9 share around 90% of identity. Eight genes, probably related to plasmid mobilization, were identified in the plasmids pZS4-9. Five of these genes encode relaxases belonging to MobA/MobL family identified by the pfam03389 conserved domain and to MOB_Q relaxase family according to the studies of de la Cruz team (Francia et al., 2004; Garcillán-Barcia et al., 2009). The next encoded relaxase belongs to the MOB_{HEN} subclade of MOB_{P5} family of relaxases (Garcillán-Barcia et al., 2009). The remaining two genes are significantly shorter than the others. One of them is classified as MobC family mobilization protein identified by the pfam05713 conserved domain and the last one encodes a putative relaxase, which we were unable to classify to a specific relaxase family. The sequences of relaxase genes located on the pZS-4, -7 and -9 plasmids are highly identical to each other (93–97%), whereas pZS-5 and pZS-6 relaxase genes share 72.4% identity. The presence of the aforementioned relaxase genes could indicate that the pZS4-9 plasmids are mobilizable replicons. Such genes were also identified in other *Acinetobacter* plasmids and the recent results obtained by Salto et al., 2018 confirm that plasmids from this group are mobilizable. In the pZS-4 plasmid sequence a tryptophan 7-halogenase gene was found, which encodes an enzyme involved in the biosynthesis of pyrrolnitrin – a broad-spectrum antifungal antibiotic.

Megaplasmids (100 kb in length and larger) constitute around 10% of all *Acinetobacter* spp. plasmids deposited in the NCBI database. Interestingly, it is suggested that environmental isolates of *Acinetobacter* spp. generally have larger plasmids than clinical ones (Salto et al., 2018). Within *A. lwoffii* species there are only six megaplasmids deposited in GenBank, all of them originating from strains isolated from permafrost and most of them being relatively similar to pmZS (a more detailed comparison of these plasmids in Section 3.2.5). For this reason, studies of plasmids from permafrost strains served as the main reference
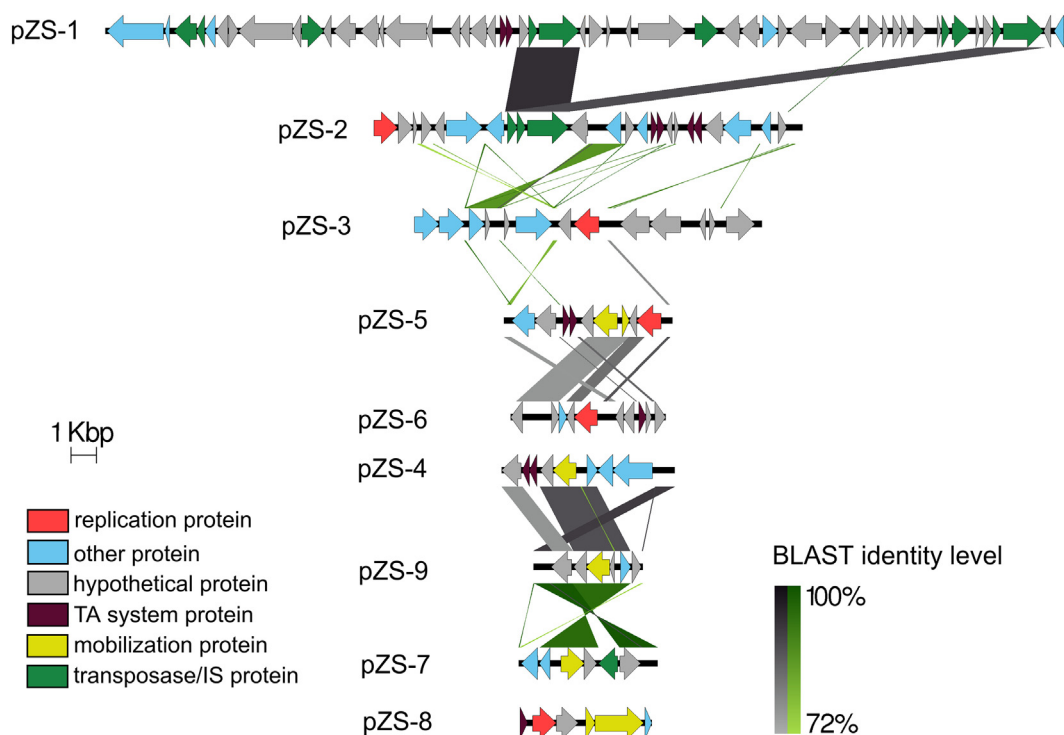
Fig. 2. Gene content and sequence identity level between smaller ZS207 strain plasmids. Arrows represent genes identified within the plasmid sequences. The direction of arrows reflects their orientation and colours show putative functions of gene products as described in the legend. Vertical blocks between the sequences indicate regions of shared similarity shaded according to BLASTn (grey to black for matches in the same direction or green for inverted matches represent sequence identity between neighbouring plasmids). The figure was generated using Easyfig application (Sullivan et al., 2011). (For interpretation of the references to colour in this figure legend, the reader is referred to the web version of this article.)

for the analysis of pmZS.

The determined sequence of pmZS megaplasmid is 186,588 bp length with 40.3% of GC content. Its nucleotide sequence is significantly similar to sequences of permafrost strains megaplasmids (Mindlin et al., 2016) covering 50–80% of its sequence with about 95% identity. Sequence analysis revealed the presence of 206 ORFs, including 47 above-mentioned transposons/IS-related genes, 3 TA systems, metal resistance genes (described in detail in Section 3.3.) and 64 hypothetical proteins genes. Among genes of predicted feature there are 11 and 9 reductase- and dehydrogenase-coding genes, respectively. All predicted genes of the pmZS megaplasmid are listed in Supplementary Table S1. The pmZS plasmid contains one incomplete prophage with ORFs assigned mostly to Stx2-converting 1717 phage. The known host of this phage is shiga-toxin-producing *Escherichia coli* O157:H7 (according to Virus-Host DB).

Other genes usually occur as individual genes, not organised in operons and encode proteins of various functions. Apart from the above mentioned pmZS genes, an exception to this rule is a complete operon for biotin biosynthesis, comprised of *bioABCDFH* genes. A *bioB* gene was also identified in the chromosomal sequence. Such operons have been reported to exist in many bacterial species, including *Acinetobacter* (Cronan, 2014) since biotin is an important cofactor for some of the enzymes involved in essential cellular pathways like the synthesis of membrane lipids or amino acid metabolism. Biotin is also required for the pathogenicity of some bacteria, such as *Mycobacterium tuberculosis* (Salaemae et al., 2016). Except for the operon for biotin biosynthesis, three neighbouring genes involved in lactate metabolism were also identified: L-lactate dehydrogenase, L-lactate permease and a regulatory protein gene. It has been reported that members of *Acinetobacter* genus are able to efficiently convert lactate to pyruvate (with L-lactate dehydrogenase), which could be used in the biotechnological pyruvate production (Allison et al., 1985; Ma et al., 2008, 2004).

Searching for genes sequences present both in plasmids and

chromosome revealed the presence of several hypothetical protein genes and transposase genes. Apart from this, some megaplasmid's genes were found also in the chromosome: already mentioned *bioB*, arsenic and metals resistance genes and *ald1*, *frmA*, *xecA1*, *rutF* encoding aldehyde dehydrogenase, glutathione dehydrogenase, 2-hydroxypropyl-CoM lyase and FMN reductase, respectively. Also, a gene encoding UvrA protein, an ATPase involved in nucleotide excision repair, was found both in the megaplasmid and chromosome. In the chromosome sequence, this gene is a part of complete *uvrABCD* operon.

3.2.2. Replication genes

An essential part of each autonomous replicon is the replication machinery, which could be recognized within its sequence. Despite extensive research into plasmid biology, including replication mechanisms, a common method or tool of simple characterization of replication mechanisms in newly described plasmids has not yet been designed. Such tools, based on the groups of incompatibility are relatively well developed for Enterobacteriaceae (Carattoli et al., 2014). Over time new approaches are proposed or the existing tools are adapted for other of bacteria. For the *Acinetobacter* genus, the classification of plasmid replication genes has only been described for *A. baumannii* (Bertini et al., 2010). This method has been successfully extended by (Salto et al., 2018) to the entire *Acinetobacter* genus.

Based on the detailed annotation, 8 ORFs involved in plasmid replication were identified, three of them on the megaplasmid. It was found that five replication initiation proteins (one from the megaplasmid and four from other plasmids - see Table S1 and Fig. 3.) belong to the Rep_B family and were assigned to the Rep_3 PFAM superfamily (pfam01051) of replication initiation proteins (Bertini et al., 2010). Following the classification scheme used by (Salto et al., 2018) (modified as described in Subsection 2.2.6), the phylogenetic analysis of the Rep_3 family proteins from ZS207 strain plasmids was performed to determine the evolutionary relationship with the corresponding

Table 3
Summary of ZS207 strain plasmidome data.

Plasmid name	Size (bp)	No. of ORFs	GC content (%)	Replication initiation proteins	Predicted maintenance and transfer genetic modules	Selected features
pZS-1	38,405	53	37.3	ND	TA system (**RelBE_1**)	Partitioning protein ParA; transposase genes (8); XerC/D recognition site
pZS-2	17,035	24	35.5	AR3G1.4	TA systems (**HigAB_2, RelBE_2**)	Transposase gene; XerC/D recognition sites (7)
pZS-3	13,816	13	35.0	AR3G2		XerC/D recognition sites (3)
pZS-4	6886	8	35.1	ND	MobA/MobL family protein, conjugal transfer protein TraD; TA system (**YafQ/DinJ_4**)	Tryptophan 7-halogenase; lysine transporter LysE
pZS-5	6691	9	34.4	AR3G8	Mobilization protein; TA system (**YafQ/RelB_5**)	LysO family lysine exporter protein; XerC/D recognition site
pZS-6	6168	11	36.3	AR3G8	MobA/MobL family protein; TA system toxin (**BrnT_6**)	XerC/D recognition sites (2)
pZS-7	5518	6	37.5	ND	MobA/MobL family protein, conjugal transfer protein TraD	Lysine transporter LysE; transposase gene
pZS-8	5246	6	37.9	replicase	Plasmid mobilization relaxosome protein MobC; TA system toxin (**relE_8**)	
pZS-9	4348	6	37.8	ND	MobA/MobL family protein, conjugal transfer protein TraD	
pmZS	186,588	206	40.3	AR3G4	TA systems (**HigBA_pm**, RelBE_pma, RelBE_pmb)	Arsenic and heavy metals resistance genes; phage replication proteins (2); plasmid partitioning - parA and parB; transposase genes (47); XerC/D recognition sites (13)

TA systems selected for plasmid stability assay are written in **bold**.

proteins from other *Acinetobacter* spp. plasmids. Within the resulting phylogenetic tree, 16 statistically supported *Acinetobacter* Rep 3 Groups (AR3G) were divided, which is consistent with the results by (Salto et al., 2018). The replication initiation protein sequences from the ZS207 strain clustered within already defined groups: pmZS sequence in AR3G4, pZS-3 in AR3G2, pZS-5 and -6 in AR3G8 and pZS-2 in AR3G1.4 group. The remaining three replication protein genes were described as replicase (pZS-8) and phage replication protein (two genes from the megaplasmid). Adjacent to megaplasmid's replication initiation gene, there are two genes involved in plasmid partitioning - *parA* and *parB*. Like in some other *Acinetobacter* plasmids, including those of *A. baumannii* (Bertini et al., 2010), putative iterons consisting of conserved direct repeats were identified upstream replication-related genes indicating their replication by the θ mechanism (Bertini et al., 2010; del Solar et al., 1998; Lean and Yeo, 2017). The *in silico* PCR-based replicon typing (PBRT) allowed to determine that pZS-2 belongs to the GR5 group of replicons according to Bertini et al., 2010 classification. Using PlasmidFinder (Carattoli et al., 2014), no plasmid replicons were found among the analyzed plasmid sequences, which is not surprising as that the program is dedicated to Enterobacteriaceae, staphylococci and streptococci. The *in silico* typing method based on the primers used to determine ST (MLST) of *A. baumannii* also did not yield any positive results. Plasmid typing schemes such as MLST or classification based on the mobility genes were shown to be difficult to apply for relatively small *Acinetobacter* replicons due to the lack of loci used in these typing schemes (Lean and Yeo, 2017). Unfortunately, no replication initiation proteins could be identified using the aforementioned methods within the sequences of pZS-1, -4, -7, and -9 plasmids.

Sixteen replication initiation proteins groups are marked in separate colours. Proteins of the ZS207 strain plasmids are indicated with a larger black label font.

To sum up, all replication genes, which were assigned to the Rep family belong to the Rep_3 superfamily. The only exceptions are two megaplasmid's genes probably of phage origin. This result is consistent with other *Acinetobacter* plasmids replicon studies, which assigned most of the replication genes to the same superfamily (Bertini et al., 2010; Lean and Yeo, 2017; Salto et al., 2018).

3.2.3. Transposable elements

A significant number of genes encoding versatile transposases and IS proteins were identified within the ZS207 strain plasmids: 47 of them in the megaplasmid sequence and 14 within the sequences of pZS-1, -2 and -7 plasmids. Among the identified genes, there are transposase genes belonging to the IS3, IS5, IS6, IS30, IS66, IS481, IS982 and ISNCY families. Genes belonging to each of above-mentioned families are present in few (2 – 11) copies, except for the single IS481 family transposase gene from the megaplasmid. All genes within each ISCNY (five genes), IS30 (two genes) and IS6 (three genes) families share almost identical nucleotide sequence. In the IS66 family, there are nine transposase genes, eight of them of very similar sequence and the remaining one being a partial transposase gene. Among the five transposase genes of the IS982 family, one differs significantly from the rest. Within both IS3 (eleven genes) and IS5 families (ten genes), three groups of almost identical genes can be distinguished. They reflect the presence of different transposase genes of the same IS family but also result from the degradation of some of them in time (contributing to the shortening of their sequence) as some transposase genes are similar but shorter than the other. The general observation is that most of the identified transposases are present in more than one copy. Almost all transposase-derived sequences located on smaller plasmids are duplicates of the megaplasmid's transposase genes. Only three short fragments of transposase genes are unique to smaller plasmids. Some transposase genes are present in more than one copy within the megaplasmid itself, sometimes as an exact copy.

There were also ten genes encoding a protein annotated as the IS66 family insertion sequence element accessory protein TnpB. According
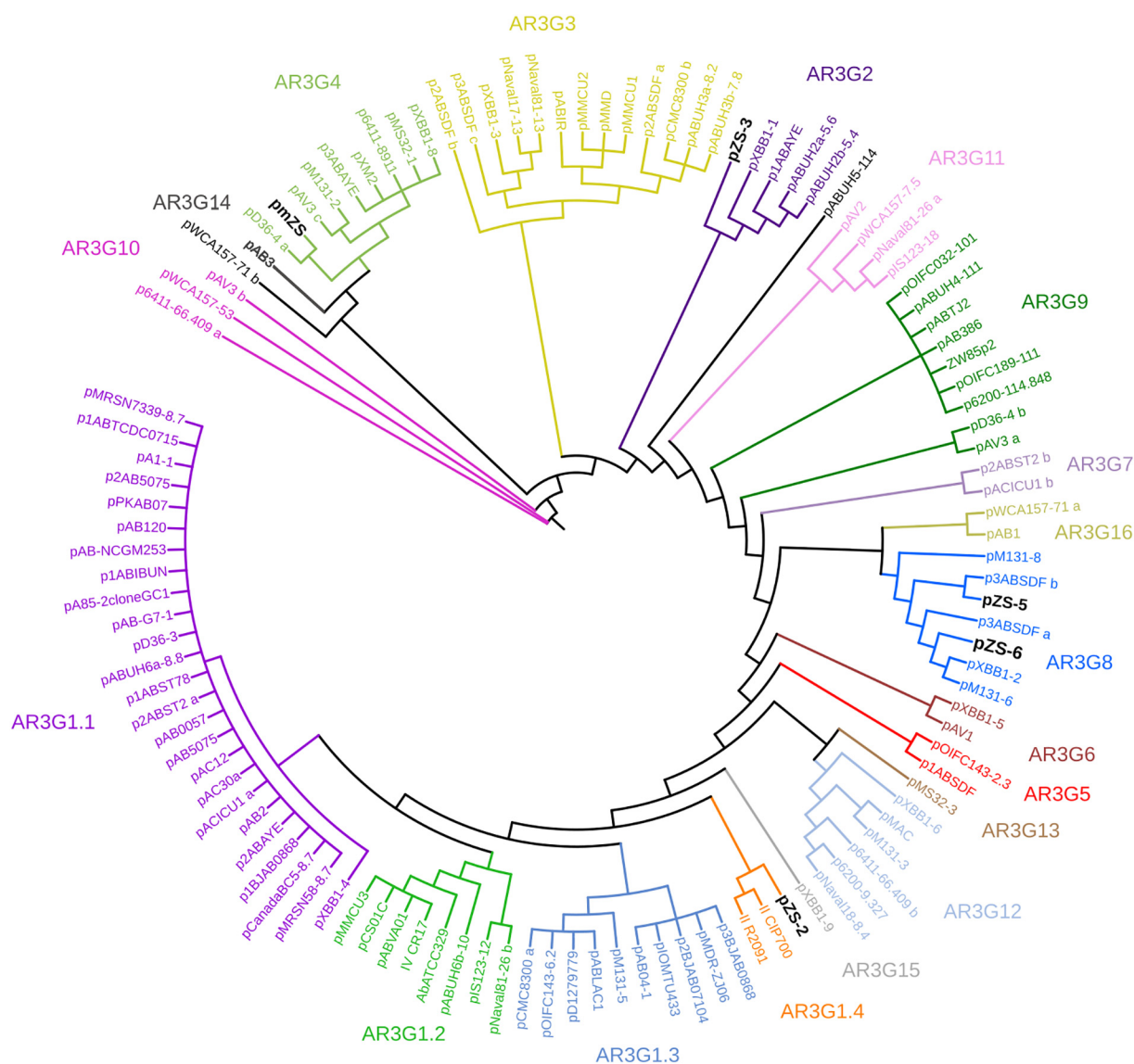
Fig. 3. Phylogenetic tree of Rep_3 domain (PF01051) replication initiation proteins from *Acinetobacter* spp. plasmids.

to the Conserved Domain Database, the function of this protein is uncertain, but they are probably essential for transposition. All genes encoding this protein share almost identical nucleotide sequence. Moreover, five genes encoding IS66 family proteins were identified, with only one being significantly different from the other.

3.2.4. XerC/D recognition sites

The Xer site-specific recombination system is highly conserved and plays a role in resolving bacterial chromosome dimers that form during DNA replication (Castillo et al., 2017). This resolution is mediated by the XerC and the XerD tyrosine recombinases. Many *Acinetobacter* plasmids contain short DNA sequences recognized by XerC/XerD site-specific tyrosine recombinases (XerC/D sites) and utilize the host Xer system to resolve their own multimeric states (Blackwell and Hall, 2017; Cameranesi et al., 2018; Mindlin et al., 2018). Moreover it is known that this system mediates in integration or excision of different mobile genetic elements to and from the host genomes (Cameranesi et al., 2018; Castillo et al., 2017). It has been proposed that the *Acinetobacter* XerC/XerD recombination system may lead to the mobilization of different DNA segments encoding adaptive features such as drug and heavy metal resistance or TA systems genes as these genes are often bordered by XerC/D sites (Brovedan et al., 2019; Mindlin et al., 2018;

Poirel and Nordmann, 2006).

XerC/D sites are generally composed by two conserved motifs of 11 bp, separated by a less-conserved central region generally spanning 6 nt (Brovedan et al., 2019) and we screened sequences of ZS207 strain plasmids for such XerC/D sites (see Section 2.2.4). This led to the identification of 27 XerC/D recognition sites among these plasmids. Such sites were present in pZS-1 (one site), pZS-2 (seven sites), pZS-3 (three sites), pZS-5 (one site), pZS-6 (two sites) and in the megaplasmid (thirteen sites). These sequences were located mainly in proximity to genes encoding hypothetical proteins or were flanking such genes. However, some of them were flanking other genes, including sulfate permease CDS, integral membrane protein CDS, a 4.2 kb region containing four genes encoding hypothetical type 1 glutamine amidotransferase, potassium transporter CDS, IS66 family transposase and two IS66 family proteins. As it can be expected the XerC/D sites were identified also in close proximity to TA systems. There were three such sites; however, all of them were found to be single. Also, one such single site was found between helix-turn-helix domain-containing protein CDS and sulfite exporter family protein CDS and one in the region with multiple transposase genes and IS-related genes.
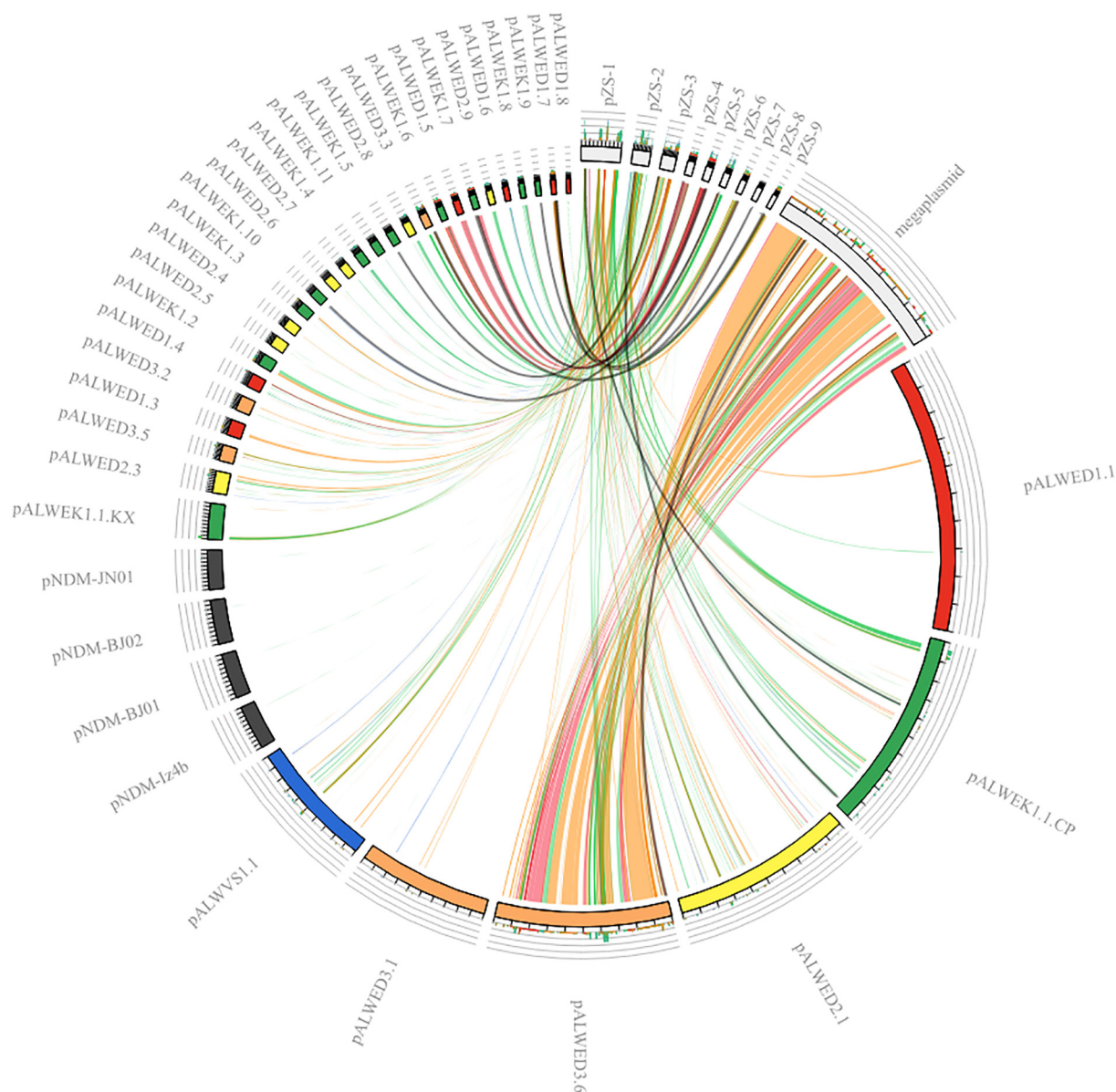
Fig. 4. Visualization of the BLAST alignment of the *A. lwoffii* ZS207 strain plasmid sequences with other selected *A. lwoffii* plasmid sequences. Bars representing the ZS207 strain plasmids are white and protrude from the circle, whereas the bars representing other *A. lwoffii* plasmids are coloured for individual hosts with the following key: yellow for ED45-23 strain, red for ED23-35, green for EK30A, orange for ED9-5a, blue for VS15 and grey for plasmids derived from clinical isolates (pNDM-BJ01 from strain WJ10621, pNDM-BJ02 from WJ10659, pNDM-Iz4b from Iz4b and pNDM-JN01 from JN49-1). Forty one strain sequences were used to calculate the similarity, 37 of them produced hits above the defined threshold. The coloured ribbons inside the circle represent regions of similarity. Particular colours reflect the defined level of sequence pairwise identity: blue ≤ 85%, green ≤ 95%, orange ≤ 99% and red above 99%. There is a histogram at the top of the ideograms counting how many times each colour has hit the specific part of the sequence. (For interpretation of the references to colour in this figure legend, the reader is referred to the web version of this article.)

3.2.5. Comparison with other A. lwoffii plasmids

The comparison of ZS207 plasmids with other *A. lwoffii* plasmids was carried out. The visualization of this analysis is shown in Fig. 4. It should be noted here that there are two plasmids named pALWEK1.1 in the GenBank database. Their length and sequence, as well as GenBank ID, are different thus we modified their names. The pALWEK1.1 of Genbank ID KX528688.1 for the purpose of this work is named pAL-WEK1.1_KX and for GenBank ID CP032102.1 we use pALWEK1.1_CP name. In the visualization, it can be seen that there are a number of smaller plasmids similar to plasmids found in the ZS207 strain as well as there is one megaplasmid highly similar to pmZS present in the studied strain, namely pALWED3.6 plasmid from the ED9-5a strain isolated from permafrost (Mindlin et al., 2016). Based on the similarity level, groups of plasmids with a different degree of identity to the

ZS207 strain plasmids can be distinguished. In particular, plasmids pALWED1.7, pALWEK1.7, pALWED1.5, pALWEK1.6 and pALWED3.3, (4.9–8.0 kb in size, also originated from permafrost strains) are highly similar to fragments of smaller ZS207 plasmids, mainly in terms of mobilization/conjugation-related, replication and TA system genes. Homologs of these genes, together with selected hypothetical protein genes are also found to a lesser extent in other *A. lwoffii* smaller plasmids from permafrost strains. The second visible group are plasmids with a low degree of similarity (pALWEK1.1_KX, pNDM-JN01, pNDM-BJ02, pNDM-Iz4b, pNDM-BJ01, pALWED3.1 and pALWED1.1; 37.5–46.6 kb and two megaplasmids) with only one or few genes similar to the ZS207 plasmid genes. These genes code almost only for transposases, several hypothetical proteins and, in pALWED3.1, also TA systems. Plasmids with names starting with pNDM- originate from
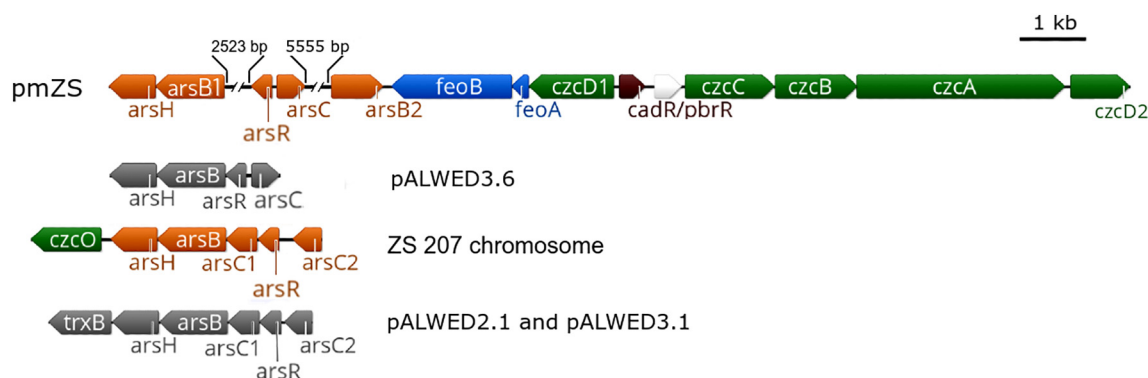
Fig. 5. The genetic organisation of the region located in the pmZS megaplasmid connected with metal(loid)s resistance.

multidrug-resistant *A. lwoffii* clinical isolates (the other from permafrost strains) and in their case, the main similarity found were IS3 family transposase genes nearly identical to those present in the plasmid pZS-1. The last group of plasmids consist of megaplasmids with genes highly similar to a variety of ZS207 plasmid genes, *i.e.* pALWEK1.1_CP, pALWED2.1, pALWED3.6 and pALWVS1.1. These megaplasmids share fragments of sequences very similar to those present in all ZS207 plasmids, except pZS-8. The genes encoded by regions similar to fragments of smaller ZS207 plasmids are mostly responsible for transposases, mobilization proteins, replication initiation proteins, TA systems and hypothetical proteins. A number of regions highly similar to the ZS207 megaplasmid sequence were also found. It should be mentioned that for clarity and due to software limitations, only the best similarity matches are shown. For this reason, some similarities are not presented, especially including the similarities between the pmZS megaplasmid and other megaplasmids: pALWEK1.1_CP, pALWED2.1, pALWED3.6 and pALWVS1.1. The sequence of the pZS-8 plasmid remains highly unique to the ZS207 strain, bearing little similarity to other *Acinetobacter* plasmids deposited in the GenBank. A search for similar sequences in the NCBI nr nucleotide database confirmed that the sequence of pZS-8 is relatively unique since there is only one significantly similar (88% identity) sequence covering 37% of pZS-8 length, derived from the p3_005046 plasmid from *A. pittii*. The plasmids pZS-1, -2 and, to some extent, pZS-3 share similarities with a relatively high number of other plasmids. This resemblance, together with the presence of several transposase genes and/or insertion sequence elements in these plasmids, can be a sign of their mosaic nature. The high similarity between the ZS207 strain plasmids and the plasmids isolated from permafrost strains can be surprising. Yet, it can be explained by the observed large-scale genetic rearrangements between different *Acinetobacter* strains as noticed by Fondi et al., 2010. It should be also noted that there are relatively few sequences of *A. lwoffii* plasmids available in NCBI database and most of them are of permafrost origin, which causes a bias in similarity searches within the *A. lwoffii* plasmid pool.

3.3. Heavy metals and arsenic resistance

The former gold and arsenic mine in Złoty Stok, from where the studied strain originates, is characterized by an elevated level of arsenic: up to 26 mg/l in waters and 30–60 mg/kg in rocks and biofilms (Drewniak et al., 2008). Other minerals extracted from the same mine contain such heavy metals as iron, lead, zinc and copper (Tomczyk-Żak et al., 2017), some of which (copper, nickel, iron or zinc) are crucial to metabolic reactions and are required by organisms as micronutrients. Others, like mercury or cadmium, play no biological role and are harmful to organisms, even in very small quantities (Sadler and Trudinger, 1967).

Microorganisms have evolved a variety of mechanisms to overcome the effect of metal(loid) toxicity, including mechanisms that restrict the entry into the cell or enable active extrusion (decreased uptake, efflux systems), enzymatic detoxification through reduction of intracellular ions (redox transformations) and intracellular chelation or precipitation (complex formation or insulation of metals) (Das et al., 2016; Gadd, 2010). Frequently metal(loid) resistance genes are located on mobile genetic elements (MGE) and can be easily transferred between different bacteria *via* horizontal gene transfer (HGT) (Sobecky and Coombs, 2009). The strains isolated from the Złoty Stok mine area commonly show arsenic resistance phenotype and the ability to transform different metal ions (Drewniak et al., 2008; Tomczyk-Żak et al., 2013).

Arsenic (As) metalloid is widely distributed in nature, occurring on four degrees of oxidation, with arsenate (+V) and arsenite (+III) being the most common. The most toxic forms of arsenic are arsenites as they cause strong bonds between functional groups, such as thiol group in the cysteine residues in cellular proteins to be formed. On the other hand, arsenates (AsO_4^{3-}), due to the similarity to phosphates (PO_4^{3-}), disturb the general cellular metabolism (Mateos et al., 2006). The most common genes conferring resistance to arsenate and arsenite are *ars* genes. *Ars* operons are widely distributed in the microbial world and they are characterized by a wide variety of gene combinations (for a review see Ben Fekih et al., 2018; Yan et al., 2019; Garbinski et al., 2019).

An *in silico* analysis of the *A. lwoffii* ZS207 plasmidome sequences revealed the presence of genes encoding resistance to arsenic salts and several heavy metals, all of them located in the same region of the pmZS megaplasmid (Fig. 5). The general organisation of this region is similar to resistance regions in the permafrost plasmids - resistance genes are mostly clustered close to each other with distinguishable modules responsible for resistance to a particular metal. However, in the permafrost plasmids, described operons contain modules giving resistance to more compounds than in pmZS.

For comparison – the organisation of the arsenic resistance operons from the chromosome of the ZS207 strain and selected plasmids of permafrost origin, namely pALWED3.6, pALWED2.1 and pALWED3.1 were included.

Arsenic resistance genes identified in the ZS207 plasmidome consist of five *ars* genes (Fig. 5 - orange ORFs). The first gene is *arsH* encoding a flavoprotein that uses $NADP^+$ to oxidize methyl As(III) to methyl As(V). Adjacent to *arsH,* there is *arsB1* gene. ArsB can associate with ArsA to form the ArsAB complex, a pump utilizing the energy of ATP hydrolysis for As(III) extrusion or it can act independently as $As(OH)_3/H^+$ antiporter that extrudes As(III), which is probably the case in ZS207, since the *arsA* gene is absent from the ZS207 genome. In the pmZS megaplasmid, *ars* genes are separated by two regions of sequence. The first one, 2523 bp in length, is located downstream from the *arsH* and *arsB1* genes and is comprised of three IS66 family proteins. Adjacent to them, there are *arsR* and *arsC* genes, coding for, respectively, a transcriptional repressor and an arsenate reductase that converts As(V) to As(III). These genes are followed by a second intrinsic sequence fragment of 5555 bp containing genes encoding an ISCNY transposase, a Fic family protein, a TerC membrane protein and an IS6 family transposase. The

last *ars* gene, which differs in size (30% shorter than the first copy) and sequence (52% of sequence identity) from the first one, is the *arsB2*. The four *ars* genes are located within a predicted prophage. The transposase gene, just before the next *ars* gene - *arsB2*, according to PHASTER results encodes a predicted phage transposase.

For each of the described *ars* genes, a number of homologs in different *Acinetobacter* species were found. The amino acid sequence identity of several best hits for each gene was above 90%. Genes identical or almost identical to the pmZS *ars* genes (except *arsB2*) were found in a recently deposited pALEWD3.6 plasmid sequence (GenBank accession number: CP032290.1), also originating from a permafrost *A. lwoffii* strain. This plasmid contains four *ars* genes (*arsHBR* and *arsC*) in the same mutual orientation in respect to the pmZS *ars* genes. The sequence identity between the pmZS and other two pALWED2.1 and pALWED3.1 permafrosts' plasmids-originated *ars* genes was 61–75%. In those plasmids, genes involved in arsenic resistance, except for *arsHBC1R* and *C2*, contain the thioredoxin reductase *trxB* (Fig. 5). In the permafrost plasmids all arsenic resistance genes are organised in an operon, while in the pmZS there are two sequence modules separating the *ars* genes. Arsenic resistance genes were also found in the chromosome of the ZS207 strain and their organisation was almost identical to the operons from pALWED2.1 and pALWED3.1 permafrost plasmids (only the *trxB* gene was missing). The sequences of chromosomal *ars* genes were also more similar to those from permafrosts strains, with 65–87% sequence identity. In contrast to the megaplasmid *ars* genes, the chromosomal *ars* operon is not located within a prophage sequence. No prophages were found in the pALWED2.1, pALWED3.1 and pA-LEWD3.6 sequences, based on which it can be suspected that the origin of the *ars* genes in the ZS207 chromosome is similar to that of the pALWED2.1 and pALWED3.1 permafrost plasmids. In contrast, the *ars* genes found in the megaplasmid probably have a different origin. This is indicated by the fact that they are located within a predicted prophage-derived sequence fragment and that the *ars* genes are separated by transposase genes. It can be assumed that individual fragments of the megaplasmid sequence containing *ars* genes were acquired in two or three independent events, perhaps as a remnant of infections of previous phage hosts.

Growth tests indicate that the detected *ars* genes are functional since the investigated *A. lwoffii* ZS207 isolate tolerates up to 30 mM and 750 mM of arsenite and arsenate, respectively, as shown below (Fig. 6). A comparative analysis of available data on arsenic resistance in identified environmental *A. lwoffii* strains (Achour et al., 2007; Das and Sarkar, 2018; Mindlin et al., 2016; Qamar et al., 2017) reveals that the ZS207 strain shows the highest resistance to arsenate and moderate tolerance to arsenite (Fig. 6).

From the observation of *A. lwoffii* ZS207 growth in the presence of arsenic ions it cannot be predicted if both, chromosomal and/or plasmid's genes are active in these processes.

To verify if *ars* genes encoded on pmZS megaplasmid contribute to the arsenic resistance, the *A. lwoffii* ZS207 selected *ars* genes were PCR amplified and then ligated into pACYC184 vector and further transferred to *E. coli* DH5α. To assess the level of resistance to both: As(V) and As(III) ions *arsC* and *arsB* genes were chosen for the analyses. As it has been mentioned, *arsC* encodes an arsenate reductase involved in the transformation of As(V) to As(III) and *arsB* encodes an integral membrane protein able to extrude As(III) from the cell. To simplify the cloning of *arsB*, the adjacent *arsH* gene was also included, but its functionality was not checked. The growth of the *E. coli* strains carrying empty pACYC184, pACYC184-arsC or pACYC184-arsBH was tested in different concentrations of As(V) or As(III). *E. coli*$_{pACYC184-arsBH}$ can grow in the presence of 7 mM concentration of arsenite, meanwhile *E. coli* carrying empty pACYC184 is only able to grow in 6 mM As(III). What is more, *E. coli*$_{pACYC184-arsC}$ survives in 150 mM As(V), while the resistance to As(V) of *E. coli* with an empty pACYC184 plasmid do not exceed 60 mM of arsenate concentration. These results suggest that both pACYC184-arsC and pACYC184-arsBH increased *E. coli* DH5α resistance to As(V) and As(III) so it can be concluded that both of the tested genes are functional.

Further *in silico* analyses also revealed the presence of three groups of genes (Fig. 5 - green, blue and brown ORFs) classified as heavy metal resistance determinants. The first group is the *czc* operon that encodes a system mediating an efflux of Co^{2+}, Zn^{2+} and Cd^{2+} ions (Silver and Phung, 2005), which in the pmZS consists of four genes encoding CzcC, B, A, and D proteins. Upstream from this operon, a single *czcD1* gene was identified. It is 381 bp longer than *czcD2* from the operon (1281 and 900 bp, respectively) and the sequence identity between these two genes is 53%. CzcC appears to modify the specificity of the system, probably by acting on the CzcB. CzcB is thought to transfer zinc cations to the CzcA, which is a cation-proton antiporter. CzcB together with CzcA can act in zinc efflux almost as effectively as the complete Czc efflux system. Moreover, CzcD mediates resistance to cobalt, cadmium and zinc *via* regulation of the Czc system. The second identified group is the *feoAB* operon that encodes a system responsible for iron transport (Lau et al., 2016). The exact role of FeoA is still unknown, but it has been postulated that FeoA plays a supporting role to FeoB in iron transport. FeoB, in turn, is a transmembrane protein that aids in the migration of iron through the membrane. The last part of the described metal resistance region is *cadR/pbrR* gene coding for a Cd(II)/Pb(II)-responsive transcriptional regulator (Brown et al., 2003).

The organisation of *czc* operon from the pmZS and the plasmids in
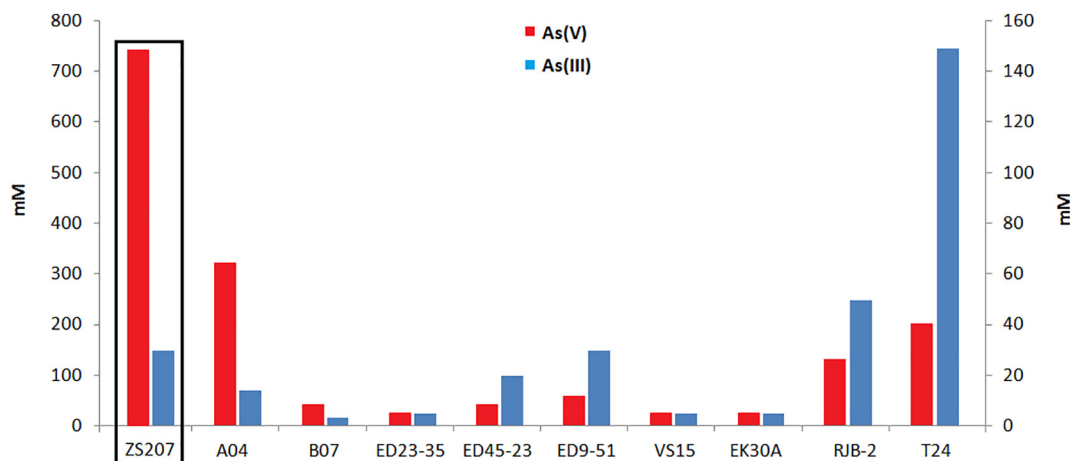

Fig. 6. Minimum inhibitory concentrations (MICs) of arsenate As(V) and arsenite As(III) against different environmental *A. lwoffii* strains including *A. lwoffii* ZS207 (first two columns in a black frame).
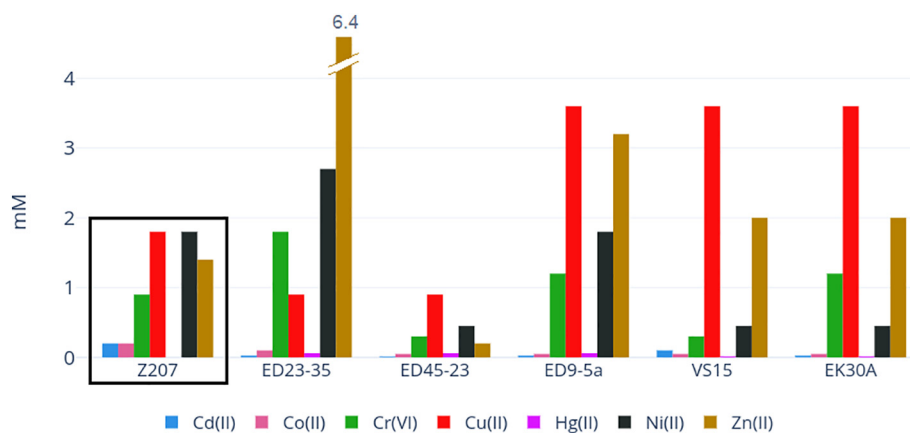
Fig. 7. Minimum inhibitory concentrations (MICs) of seven heavy metals against different environmental *A. lwoffii* strains including *A. lwoffii* ZS207 (columns in black frame).

permafrost strains (pALWED3.1, pALWED1.1, pALWVS1.1 and pALWEK1.1) is nearly identical. The only difference is the presence of *czcD2* gene in the pmZS sequence. The sequence identity of *czc* genes is also very high compared to permafrost plasmids and is at the level of 94–99%. The only exceptions are *czcA, B* and *C* genes from the pALWED3.1 plasmid, which differ from the genes of other compared operons to a higher degree (51–70% of sequence identity).

The presence of predicted metal resistance genes prompted us to test the ZS207 strain resistance to cobalt, zinc and cadmium. Additionally, resistance to chromium, copper, nickel and mercury was tested. These four metals were included in the experiment because we eventually wanted to compare ZS207 heavy metal resistance with the level of resistance in permafrost *A. lwoffii* isolates (Mindlin et al., 2016), the only environmental strains described so far, which, among others, were also characterized in terms of metal resistance to these seven metal compounds.

The obtained results revealed a great deal of variation in the resistance pattern of the isolate to each metal ion studied (Fig. 7). The bacterium showed relatively high resistance to copper and nickel (1.8 mM), moderate resistance to zinc and chromium (1.4 and 0.9 mM, respectively) and low resistance to cobalt and cadmium (0.2 mM). The strain ZS207 exhibits a sensitive phenotype only in the presence of mercury, even when applied in the lowest (0.015 mM) tested dose.

Heavy metal resistance tests show that *A. lwoffii* ZS207 exhibits a higher resistance level to cadmium and cobalt than all the permafrost *A. lwoffii* strains (Fig. 7). This can be explained by the fact that the genes involved in mediating an efflux of these compounds were identified not only in the ZS207 megaplasmid but also in the chromosome, where a preliminary analysis revealed the presence of genes involved in cobalt and cadmium resistance (*czcA, czcD, czcO* and *czcRS*). Additionally, a number of genes related to other heavy metal resistance were identified in the chromosome; for example, *modABC* operon (molybdenum resistance), *copAB, cueR* (copper resistance), *srpC* (chromium resistance), *feoA, feoB* (iron transport), *zupT, znuA, znuCB,* and *zur* (zinc resistance). This could provide an explanation of copper, chromium and zinc resistance in the ZS207 strain despite the absence of corresponding genes on its plasmids.

3.4. TA genes

The analysis of the content of the plasmids showed that they encode several potential TA systems. The presence of mechanisms leading to plasmid maintenance is not surprising as there are 10 extra-chromosomal replicons in the strain, nine of which appear to be cryptic plasmids. The TA systems in relatively small *Acinetobacter* Rep_3 plasmids are common and were shown to be functional in some clinical isolates (Armalytė et al., 2018; Ghafourian et al., 2014; Jurenaite et al.,

2013; Lean and Yeo, 2017). A multitude of TA systems combined with the presence of several IS- or transposon-related genes also reflects genome plasticity of a given strain. Therefore, a closer look at the toxin- and antitoxin-coding genes was taken to estimate the completeness and classification of TA systems to a defined group.

3.4.1. In silico analysis

Because the degree of sequence identity between toxin genes and antitoxin genes from the same family is rather low, the *A. lwoffii* ZS207 TA systems were curated manually by bioinformatic work followed by an experimental approach.

Eight complete plasmid-encoded TA systems (Table 3, Table S1) were identified, all of them belonging to type II TA systems, either HigBA or RelBE superfamily modules. The activity of all toxins from those operons is based on an mRNA cleavage mechanism. Three TA operons are located on the pmZS megaplasmid, two of them on the pZS-2 plasmid and the remaining three on the pZS-1, pZS-4, and pZS-5 plasmids, with one TA operon on each of them. Apart from the above-mentioned TA systems, two putative chromosomal-encoded TA operons (HipAB and GNAT toxin with RelB/DinJ family antitoxin) and seven individual toxin- or antitoxin-coding genes were identified, two of which located on plasmids (Supplementary Table S1).

It was found that in the RelBE_2, RelBE_pma and RelBE_pmb modules both the nucleotide and translated sequence of toxin and antitoxin genes are almost identical. The aa sequence identity of RelBE_1 to the three above-mentioned ones is much lower, namely 44% (64% positives) for translated toxin genes, and around 20% for translated antitoxin sequences. At the same time, the identity of the translated YafQ/RelB_5 and YafQ/DinJ_4 is 57% for toxins and 48% for antitoxin with 74% and 68% positives, respectively. In the HigBA_2 and HigBA_pm operons, the level of sequence identity is very low (below 20%). The RelE/ParE gene from the pZS-8 plasmid shows marginal similarity to other RelE/ParE genes.

The search for homologs of the ZS207 TA genes revealed the presence of almost identical sequences in many other *Acinetobacter* members.

3.4.2. Stabilization potential examination

Active TA systems from plasmids ensure plasmid maintenance in growing bacterial populations by killing plasmid-free segregants that have lost the plasmid at the time of cell division, a phenomenon known as post-segregational killing (PSK) (Gerdes et al., 1986). Stabilizing properties of TA systems are observed in low-copy antibiotic resistance-carrying plasmids as a maintenance mechanism of antibiotic resistance in cells growing in the absence of an antibiotic as a selective pressure. When a TA system is not functional, there is no PSK so the lack of the plasmid does not affect the viability of daughter cells. Its absence will

result in a loss of antibiotic resistance in non-selective conditions, which can be easily observed.

Six TA systems located on the plasmids of the ZS207 strain were selected for further analysis (indicated in Table 3 and Table 2). Since three identified RelBE operons were almost identical, only one from that group, namely RelBE_2 from pZS-2, was chosen for *in-vitro* experiments. To assess the functionality of plasmid-encoded TA systems identified *in silico*, corresponding DNA fragments amplified by PCR were cloned into the pABB35 plasmid and the stability of the pABB35 derivatives was tested in *E. coli*. The pABB35 vector is a single-copy, highly unstable, broad-host-range plasmid based on the RK2 replicon of the IncP-1 group (Pansegrau et al., 1994), which was designed to test stabilization functions in various bacterial species. The high instability of pABB35 in *E. coli* was confirmed and described in (Bartosik et al., 2016). The sequences of all fragments cloned into the pABB35 derivatives were verified by Sanger sequencing and compared with those revealed by the genome assembly. No differences between cloned and NGS sequences were detected in any case, additionally confirming the high level of sequencing strategy and data handling.

The functionality of the TA systems was estimated by assessing the effect of operons cloned into pABB35 on the vector retention in growing *E. coli* population by the standard plasmid stabilization assay (Methods 2.4.). *Acinetobacter* and *Escherichia* belong to the same Gammaproteobacteria class suggesting a high probability of proper expression of the cloned ZS207 sequences.

The differences in the stabilization potential reflect the individual functionality of each TA system. Plasmid stability tests showed that all studied TA systems: HigBA_pm, HigBA_2, YafQ/DinJ_4, YafQ/RelBE_5, RelBE_1, and RelBE_2 greatly improved pABB35 plasmid segregation rate. As shown in Fig. 8 - from 85 to 100% of *E. coli* DH5α cells retained the plasmid under non-selective conditions (LB medium without antibiotics) until generation 16. What is more, all of the tested TA systems keep their stabilizing properties even until generation 30 (see Supplementary Fig. S2.); however in the case of HigBA_pm, HigBA_2 and RelBE_2 the stabilization effect is slightly decreasing with time - so that at the end of the experiment plasmids were present in around 70% of cells carrying HigBA_pm and RelBE_2 and in 60% of cells carrying HigBA_2 operon. On the other hand, for the *E. coli* population carrying an empty pABB35 plasmid only around 20% of the cells retained the vector after 30 generations.

Additionally, a more in-depth analysis of unaccompanied BrnT_6 toxin encoded on the pZS-6 plasmid was carried out. Knowing that

cloning of a functional toxin is nearly impossible in the absence of the cognate antitoxin we wanted to assess whether BrnT_6 is actually active. If it was not – its cloning and transformation of *E. coli* cells would be successful. Because *E. coli* transformants carrying pGEM with *brnT_6* were obtained, it seems that BrnT_6 is not functional, or *E. coli* cells do not contain a target site recognized by *A. lwoffii* BrnT_6, or its toxic effect is neutralized by another antitoxin/s present in the cells. The third scenario seems to be the most probable as BrnT belongs to the same RelE toxin family as many other *E. coli* and *A. lwoffii* TA toxins. It was shown that BrnT is capable of binding not only to cognate BrnA, but also structurally disparate antitoxins (Heaton et al., 2012).

The functionality of another identified orphan toxin, RelE_8, was not verified experimentally although an *in silico* analysis revealed that this toxin exhibits a rather low similarity to other RelE toxins encoded in the *A. lwoffii* ZS207 plasmidome. Again, we reasoned that it is highly probable that even if it is functional, its activity is neutralized by multiple antitoxins from other RelBE TA systems present in the cell.

3.4.3. Persister cells

All investigated toxin-antitoxin systems of *A. lwoffii* ZS207 belong to class II family of *bona fide* proteic TAs in which both components are proteins (Díaz-Orejas et al., 2017; Leplae et al., 2011; Page and Peti, 2016). Its functioning is based on different decay rates of two proteins involved: toxins are much more stable than antidotes. Antitoxins neutralize their cognate toxins by forming tight toxin-antitoxin complexes. Different stress conditions (or the loss of the plasmid carrying the TA cassette) lead to the activation of TA systems: the rapid decay of labile antitoxin liberates non-neutralized toxin, which inhibits cell growth by targeting essential cellular processes (Gerdes et al., 2005; Hayes and Van Melderen, 2011; Jurėnas et al., 2017).

When an isogenic bacterial population is treated with high doses of bactericidal antibiotics, a small fraction survives. These so-called persister cells are not genetic mutants but phenotypic variants (Balaban et al., 2004; Lewis, 2010; Moyed and Bertrand, 1983). These non-dividing cells can survive exposure to different kinds of stress, such as high temperature or antibiotics. Once relieved from quiescence, the persisters return to the state, in which they are able to grow and they repopulate the environment.

Earlier studies have been showing toxin-antitoxin modules to be implicated in the induction of persistence (Falla and Chopra, 1998; Keren et al., 2004; Page and Peti, 2016). Toxins of TA systems inhibit essential cellular functions, leading to cells switching into the persister state. However, most recent literature reports a controversy in the validity of many published results concerning TA-dependent persister cells formation (Goormaghtigh et al., 2018; Ronneau and Helaine, 2019), including a retraction of several significant papers (*e.g.*: Maisonneuve et al., 2011; Germain et al., 2015). This current disputation was an inspiration to study if TA systems in *Acinetobacter*, a strain not studied in this respect yet, could be linked to the persistence.

The presence of multiple functional TA systems in the studied *Acinetobacter* strain prompted us to check whether *A. lwoffii* ZS207 subjected to stress conditions will form an elevated level of antibiotic-tolerant persisters in comparison with non-stressed bacteria. The adopted strategy is based on the assumption that applying sharp intensive stress will physiologically turn on at least some of TAs and, as a consequence of their activity, will lead to the persister cells formation.

Firstly, the viability of the isolate after being treated with the given stress conditions was checked. After confirming that the cells are able to survive, the main experiments were conducted. Surprisingly, NaCl stress had no effect on drug tolerance, so in further experiments, only the effect of thermal stress on persister formation was tested.

Both examined cultures, treated and not treated with high temperature (60 °C, 20 min), were afterwards exposed to ampicillin for 4 h (in optimal growth conditions). The comparison of these two tested cultures shows that there is an increase in the survival of the temperature-stressed cells compared to non-stressed ones (after exposure to
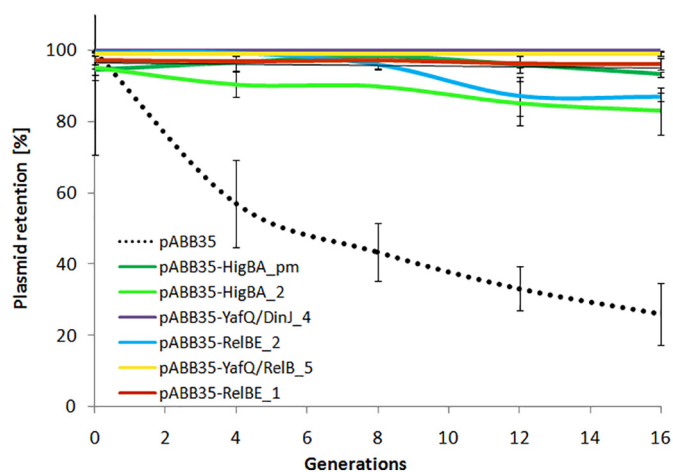
Fig. 8. The stabilization effect of *A. lwoffii* ZS207 TA systems cloned into the pABB35 vector introduced into *E. coli* DH5α, propagated for 16 generations. The figure presents outputs from a standard stabilization assay with the use of replica plating to estimate the proportion of colonies retaining the tested plasmids (conferring resistance to chloramphenicol). The results show the mean from at least three independent experiments with standard deviation.
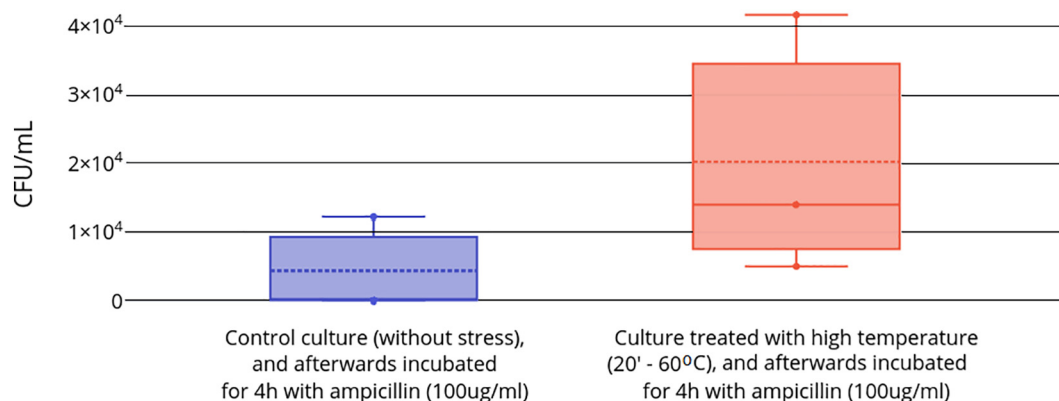
Fig. 9. Effects of thermal stress on persister formation in the wild-type *A. lwoffii* ZS207 strain. Persister assay results showing the survival of bacteria with respect to 4 h pre-antibiotic treatment. Error bars indicate standard deviation from the mean ($n = 3$).

ampicillin). In the three consecutive experiments thermal stress discriminately caused an increase in the level of persister formation to 2.7-fold (Fig. 9). However, it is not statistically significant. Moreover, taking into consideration all conducted experiment repetitions (including different experiments performers and time intervals) only 1.6-fold increase in a number of persisters was observed (see Supplements - Fig. S3), so, in fact, there are no premises proving that temperature stress may promote an intensified formation of antibiotic-tolerant persisters. In addition, no increase in persister cell formation was observed, when cultures were exposed to another antibiotic (streptomycin 100 μg/ml).

On the whole, the formation of persister cells linked to TA systems is observed in the following types of experiments: involving over-expression of toxins (Correia et al., 2006; Keren et al., 2004; Korch et al., 2003) or using isogenic strains, in which TAs were knocked-out (Gross et al., 2006; Keren et al., 2004). In our study, a 'natural' state of cells without over- or under-expression of TA systems was used. It was expected that the application of a sharp intensive stress will physiologically turn on at least some of multiple TAs present in the studied strain and, as a consequence of their activity, will lead to the persister cell formation. It turns out that the obtained results were not entirely conclusive.

A detailed re-analysis of already performed experimental works for *E. coli* and several other bacteria suggests TA systems are not directly responsible for persistence and emphasizes that the currently applied methodology might not be suitable enough for persistence research (Fraikin et al., 2019). For this reason, it cannot be excluded that the observed low 'efficacy' of persister cell formation in the experiments on the *A. lwoffii* ZS207 strain is, among others, a consequence of the conditions and/or limitations of the methodology, which makes persister cell formation studies technically challenging.

4. Conclusions

One megaplasmid and nine smaller plasmids were shown to co-exist in an environmental isolate of *A. lwoffii* — ZS207. Plasmids in the ZS207 strain share a number of highly identical regions. Most of them occur between the megaplasmid, pZS-1 and pZS-2. Overall, ZS207 strain plasmids show significant similarity with plasmids isolated from permafrost *A. lwoffii* strains. In the light of the isolation sites of the permafrost strains and the ZS207 strain, such level of similarity is surprising. Together with the presence of many transposase genes, it indicates a high level of genomic plasticity and genetic rearrangements taking place between different *A. lwoffii* strains as has been repeatedly shown for the whole *Acinetobacter* genus.

The pmZS megaplasmid carries genes encoding arsenic and heavy metal resistant determinants. The rest of the plasmids seem not to encode genes that contribute to the phenotype of the ZS207 isolate. The *in*

silico analysis of the ZS207 plasmidome revealed the existence of eight potential complete toxin-antitoxin systems. All experimentally tested *A. lwoffii* ZS207 TA systems are functional and since 9 of 10 plasmids appear to have an unknown benefit to the host cell, it is highly probable that identified TA systems are involved in the maintenance of the ZS207 plasmids. TA systems were also commonly associated with promoting a transition to a dormant state, but evident persister cells formation was not observed in *A. lwoffii* ZS207. The strain exhibits high tolerance to arsenite (30 mM) and arsenate (750 mM) as well as to cadmium and cobalt in comparison with other environmental *A. lwoffii* isolates described in the current literature, which makes it potentially useful in bioremediation of arsenic and selected other heavy metals.

Note

At the time of the manuscript re-submission the complete genome sequence of the *A. lwoffii* FDAARGOS_552 strain was deposited in the NCBI database (BioSample SAMN10163245). Its nucleotide sequence shows high similarity with ZS207 both, chromosome (97% of overall BLAST sequence identity on 87% of query length) and megaplasmid (98% of overall BLAST sequence identity on 75% of query length). The 6691 bp length unnamed plasmid from FDAARGOS_552 strain is virtually identical to pZS-5, except two single residues.

CRediT authorship contribution statement

Urszula Zielenkiewicz: Conceptualization, Methodology, Supervision, Writing, Funding Acquisition. **Marcin Jurkowski:** Investigation, Reviewing and Editing. **Tomasz Walter:** Software, Data curation, Visualization. Writing- Original draft preparation. **Joana Klim:** Investigation, Visualization, Writing-Original draft preparation. **Iwona Brzozowska-Köhling:** Investigation, Methodology, Supervision. **Małgorzata Słodownik:** Investigation.

Appendix A. Supplementary data

References

Achour, A.R., Bauda, P., Billard, P., 2007. Diversity of arsenite transporter genes from arsenic-resistant soil bacteria. Res. Microbiol. 158, 128–137. https://doi.org/10.1016/j.resmic.2006.11.006.

Allison, N., O'Donnell, M.J., Hoey, M.E., Fewson, C.A., 1985. Membrane-bound lactate dehydrogenases and mandelate dehydrogenases of *Acinetobacter calcoaceticus*. Location and regulation of expression. Biochem. J. 227, 753–757.

Altschul, S.F., Gish, W., Miller, W., Myers, E.W., Lipman, D.J., 1990. Basic local alignment search tool. J. Mol. Biol. 215, 403–410. https://doi.org/10.1016/S0022-2836(05)80360-2.

Armalytė, J., Jurėnas, D., Krasauskas, R., Čepauskas, A., Sužiedėlienė, E., 2018. The higBA toxin-antitoxin module from the opportunistic pathogen *Acinetobacter baumannii* - regulation, activity, and evolution. Front. Microbiol. 9, 732. https://doi.org/10.3389/fmicb.2018.00732.

Arndt, D., Grant, J.R., Marcu, A., Sajed, T., Pon, A., Liang, Y., Wishart, D.S., 2016. PHASTER: a better, faster version of the PHAST phage search tool. Nucleic Acids Res. 44, W16–W21. https://doi.org/10.1093/nar/gkw387.

Aziz, R.K., Bartels, D., Best, A.A., DeJongh, M., Disz, T., Edwards, R.A., Formsma, K., Gerdes, S., Glass, E.M., Kubal, M., Meyer, F., Olsen, G.J., Olson, R., Osterman, A.L., Overbeek, R.A., McNeil, L.K., Paarmann, D., Paczian, T., Parrello, B., Pusch, G.D., Reich, C., Stevens, R., Vassieva, O., Vonstein, V., Wilke, A., Zagnitko, O., 2008. The RAST Server: rapid annotations using subsystems technology. BMC Genomics 9, 75. https://doi.org/10.1186/1471-2164-9-75.

Balaban, N.Q., Merrin, J., Chait, R., Kowalik, L., Leibler, S., 2004. Bacterial persistence as a phenotypic switch. Science 305, 1622–1625. https://doi.org/10.1126/science.1099390.

Bartosik, A.A., Glabski, K., Kulinska, A., Lewicka, E., Godziszewska, J., Markowska, A., Jagura-Burdzy, G., 2016. Convenient broad-host-range unstable vectors for studying stabilization cassettes in diverse bacteria. BMC Microbiol. 16, 59. https://doi.org/10.1186/s12866-016-0674-y.

Ben Fekih, I., Zhang, C., Li, Y.P., Zhao, Y., Alwathnani, H.A., Saquib, Q., Rensing, C., Cervantes, C., 2018. Distribution of arsenic resistance genes in prokaryotes. Front. Microbiol. 9. https://doi.org/10.3389/fmicb.2018.02473.

Bertini, A., Poirel, L., Mugnier, P.D., Villa, L., Nordmann, P., Carattoli, A., 2010. Characterization and PCR-based replicon typing of resistance plasmids in *Acinetobacter baumannii*. Antimicrob. Agents Chemother. 54, 4168–4177. https://doi.org/10.1128/AAC.00542-10.

Blackwell, G.A., Hall, R.M., 2017. The tet39 determinant and the msrE-mphE genes in acinetobacter plasmids are each part of discrete modules flanked by inversely oriented pdif (XerC-XerD) sites. Antimicrob. Agents Chemother. 61. https://doi.org/10.1128/AAC.00780-17.

Brovedan, M., Repizo, G.D., Marchiaro, P., Viale, A.M., Limansky, A., 2019. The plasmid diversity of *Acinetobacter bereziniae* HPC229 provides clues on the ability of the species to thrive on both clinical and environmental habitats. bioRxiv 710913. https://doi.org/10.1101/710913.

Brown, N.L., Stoyanov, J.V., Kidd, S.P., Hobman, J.L., 2003. The MerR family of transcriptional regulators. FEMS Microbiol. Rev. 27, 145–163. https://doi.org/10.1016/S0168-6445(03)00051-2.

Cameranesi, M.M., Morán-Barrio, J., Limansky, A.S., Repizo, G.D., Viale, A.M., 2018. Site-specific recombination at XerC/D sites mediates the formation and resolution of plasmid co-integrates carrying a blaOXA-58- and TnaphA6-resistance module in *Acinetobacter baumannii*. Front. Microbiol. 9. https://doi.org/10.3389/fmicb.2018.00066.

Carattoli, A., Zankari, E., García-Fernández, A., Voldby Larsen, M., Lund, O., Villa, L., Møller Aarestrup, F., Hasman, H., 2014. In silico detection and typing of plasmids using PlasmidFinder and plasmid multilocus sequence typing. Antimicrob. Agents Chemother. 58, 3895–3903. https://doi.org/10.1128/AAC.02412-14.

Castillo, F., Benmohamed, A., Szatmari, G., 2017. Xer site specific recombination: double and single recombinase systems. Front. Microbiol. 8. https://doi.org/10.3389/fmicb.2017.00453.

Colston, S.M., Fullmer, M.S., Beka, L., Lamy, B., Gogarten, J.P., Graf, J., 2014. Bioinformatic genome comparisons for taxonomic and phylogenetic assignments using Aeromonas as a test case. MBio 5, e02136. https://doi.org/10.1128/mBio.02136-14.

Correia, F.F., D'Onofrio, A., Rejtar, T., Li, L., Karger, B.L., Makarova, K., Koonin, E.V., Lewis, K., 2006. Kinase activity of overexpressed HipA is required for growth arrest and multidrug tolerance in *Escherichia coli*. J. Bacteriol. 188, 8360–8367. https://doi.org/10.1128/JB.01237-06.

Cronan, J.E., 2014. Biotin and Lipoic Acid: Synthesis, Attachment and Regulation. 6 EcoSal Plus https://doi.org/10.1128/ecosalplus.ESP-0001-2012.

Darriba, D., Taboada, G.L., Doallo, R., Posada, D., 2011. ProtTest 3: fast selection of best-fit models of protein evolution. Bioinformatics 27, 1164–1165. https://doi.org/10.1093/bioinformatics/btr088.

Darzentas, N., 2010. Circoletto: visualizing sequence similarity with Circos. Bioinformatics 26, 2620–2621. https://doi.org/10.1093/bioinformatics/btq484.

Das, J., Sarkar, P., 2018. Remediation of arsenic in mung bean (*Vigna radiata*) with growth enhancement by unique arsenic-resistant bacterium *Acinetobacter lwoffii*. Sci. Total Environ. 624, 1106–1118. https://doi.org/10.1016/j.scitotenv.2017.12.157.

Das, S., Dash, H.R., Chakraborty, J., 2016. Genetic basis and importance of metal resistant genes in bacteria for bioremediation of contaminated environments with toxic metal pollutants. Appl. Microbiol. Biotechnol. 100, 2967–2984. https://doi.org/10.1007/s00253-016-7364-4.

Díaz-Orejas, R., Espinosa, M., Yeo, C.C., 2017. The importance of the expendable: toxin-antitoxin genes in plasmids and chromosomes. Front. Microbiol. 8, 1479. https://doi.org/10.3389/fmicb.2017.01479.

Dörr, T., Vulić, M., Lewis, K., 2010. Ciprofloxacin causes persister formation by inducing the TisB toxin in *Escherichia coli*. PLoS Biol. 8, e1000317. https://doi.org/10.1371/journal.pbio.1000317.

Drewniak, L., Styczek, A., Majder-Lopatka, M., Sklodowska, A., 2008. Bacteria, hypertolerant to arsenic in the rocks of an ancient gold mine, and their potential role in dissemination of arsenic pollution. Environ. Pollut. 156, 1069–1074. https://doi.org/10.1016/j.envpol.2008.04.019.

Dworkin, M., Falkow, S., Rosenberg, E., Schleifer, K.-H., Stackebrandt, E. (Eds.), 2006. The Prokaryotes: Vol. 6: Proteobacteria: Gamma Subclass, 3rd ed. Springer-Verlag, New York.

Falla, T.J., Chopra, I., 1998. Joint tolerance to β-lactam and fluoroquinolone antibiotics in *Escherichia coli* results from overexpression of hipA. Antimicrob. Agents Chemother. 42, 3282–3284. https://doi.org/10.1128/AAC.42.12.3282.

Fondi, M., Bacci, G., Brilli, M., Papaleo, M.C., Mengoni, A., Vaneechoutte, M., Dijkshoorn, L., Fani, R., 2010. Exploring the evolutionary dynamics of plasmids: the Acinetobacter pan-plasmidome. BMC Evol. Biol. 10, 59. https://doi.org/10.1186/1471-2148-10-59.

Fraikin, N., Goormaghtigh, F., Van Melderen, L., 2019. Toxin-antitoxin systems and persistence. In: Lewis, K. (Ed.), Persister Cells and Infectious Disease. Springer International Publishing, Cham, pp. 181–202. https://doi.org/10.1007/978-3-030-25241-0_8.

Francia, M.V., Varsaki, A., Garcillán-Barcia, M.P., Latorre, A., Drainas, C., de la Cruz, F., 2004. A classification scheme for mobilization regions of bacterial plasmids. FEMS Microbiol. Rev. 28, 79–100. https://doi.org/10.1016/j.femsre.2003.09.001.

Gadd, G.M., 2010. Metals, minerals and microbes: geomicrobiology and bioremediation. Microbiology 156, 609–643. https://doi.org/10.1099/mic.0.037143-0.

Garbinski, L.D., Rosen, B.P., Chen, J., 2019. Pathways of arsenic uptake and efflux. Environ. Int. 126, 585–597. https://doi.org/10.1016/j.envint.2019.02.058.

Garcillán-Barcia, M.P., Francia, M.V., Cruz, F.D.L., 2009. The diversity of conjugative relaxases and its application in plasmid classification. FEMS Microbiol. Rev. 33, 657–687. https://doi.org/10.1111/j.1574-6976.2009.00168.x.

Garrity, G., De Vos, P., 2005. Genus Acinetobacter. In: Bergey's Manual of Systematic Bacteriology. Springer, pp. 425–437.

Gerdes, K., Bech, F.W., Jørgensen, S.T., Løbner-Olesen, A., Rasmussen, P.B., Atlung, T., Boe, L., Karlstrom, O., Molin, S., von Meyenburg, K., 1986. Mechanism of post-segregational killing by the hok gene product of the parB system of plasmid R1 and its homology with the relF gene product of the E. coli relB operon. EMBO J. 5, 2023–2029.

Gerdes, K., Christensen, S.K., Løbner-Olesen, A., 2005. Prokaryotic toxin-antitoxin stress response loci. Nat. Rev. Microbiol. 3, 371–382. https://doi.org/10.1038/nrmicro1147.

Germain, E., Roghanian, M., Gerdes, K., Maisonneuve, E., 2015. Stochastic induction of persister cells by HipA through (p)ppGpp-mediated activation of mRNA endonucleases. PNAS 112, 5171–5176. https://doi.org/10.1073/pnas.1423536112.

Ghafourian, S., Good, L., Sekawi, Z., Hamat, R.A., Soheili, S., Sadeghifard, N., Neela, V., 2014. The mazEF toxin-antitoxin system as a novel antibacterial target in *Acinetobacter baumannii*. Mem. Inst. Oswaldo Cruz 109, 502–505.

Goormaghtigh, F., Fraikin, N., Putrinš, M., Hallaert, T., Hauryliuk, V., Garcia-Pino, A., Sjödin, A., Kasvandik, S., Udekwu, K., Tenson, T., Kaldalu, N., Melderen, L.V., 2018. Reassessing the role of type II toxin-antitoxin systems in formation of *Escherichia coli* type II Persister cells. mBio 9 https://doi.org/10.1128/mBio.00640-18. e00640–18.

Goris, J., Konstantinidis, K.T., Klappenbach, J.A., Coenye, T., Vandamme, P., Tiedje, J.M., 2007. DNA-DNA hybridization values and their relationship to whole-genome sequence similarities. Int. J. Syst. Evol. Microbiol. 57, 81–91. https://doi.org/10.1099/ijs.0.64483-0.

Gross, M., Marianovsky, I., Glaser, G., 2006. MazG—a regulator of programmed cell death in *Escherichia coli*. Mol. Microbiol. 59, 590–601. https://doi.org/10.1111/j.1365-2958.2005.04956.x.

Guindon, S., Dufayard, J.-F., Lefort, V., Anisimova, M., Hordijk, W., Gascuel, O., 2010. New algorithms and methods to estimate maximum-likelihood phylogenies: assessing the performance of PhyML 3.0. Syst. Biol. 59, 307–321. https://doi.org/10.1093/sysbio/syq010.

Hanahan, D., 1983. Studies on transformation of *Escherichia coli* with plasmids. J. Mol. Biol. 166, 557–580. https://doi.org/10.1016/s0022-2836(83)80284-8.

Hayes, F., Van Melderen, L., 2011. Toxins-antitoxins: diversity, evolution and function. Crit. Rev. Biochem. Mol. Biol. 46, 386–408. https://doi.org/10.3109/10409238.2011.600437.

Heaton, B.E., Herrou, J., Blackwell, A.E., Wysocki, V.H., Crosson, S., 2012. Molecular structure and function of the novel BrnT/BrnA toxin-antitoxin system of *Brucella abortus*. J. Biol. Chem. 287, 12098–12110. https://doi.org/10.1074/jbc.M111.332163.

Hu, Y., Zhang, W., Liang, H., Liu, L., Peng, G., Pan, Y., Yang, X., Zheng, B., Gao, G.F., Zhu, B., Hu, H., 2011. Whole-genome sequence of a multidrug-resistant clinical isolate of *Acinetobacter lwoffii*. J. Bacteriol. 193, 5549–5550. https://doi.org/10.1128/JB.05617-11.

Imperi, F., Antunes, L.C.S., Blom, J., Villa, L., Iacono, M., Visca, P., Carattoli, A., 2011. The genomics of *Acinetobacter baumannii*: insights into genome plasticity, antimicrobial resistance and pathogenicity. IUBMB Life 63, 1068–1074. https://doi.org/10.1002/iub.531.

Jurenaite, M., Markuckas, A., Suziedeliene, E., 2013. Identification and characterization of type II toxin-antitoxin systems in the opportunistic pathogen *Acinetobacter baumannii*. J. Bacteriol. 195, 3165–3172. https://doi.org/10.1128/JB.00237-13.

Jurėnas, D., Garcia-Pino, A., Van Melderen, L., 2017. Novel toxins from type II toxin-antitoxin systems with acetyltransferase activity. Plasmid 93, 30–35. https://doi.org/10.1016/j.plasmid.2017.08.005.

Kämpfer, P., 2014. Acinetobacter. In: Batt, C.A., Tortorello, M.L. (Eds.), Encyclopedia of Food Microbiology, Second edition. Academic Press, Oxford, pp. 11–17. https://doi.org/10.1016/B978-0-12-384730-0.00002-1.

Keren, I., Shah, D., Spoering, A., Kaldalu, N., Lewis, K., 2004. Specialized persister cells and the mechanism of multidrug tolerance in *Escherichia coli*. J. Bacteriol. 186, 8172–8180. https://doi.org/10.1128/JB.186.24.8172-8180.2004.

Koonin, E.V., Wolf, Y.I., 2008. Genomics of bacteria and archaea: the emerging dynamic view of the prokaryotic world. Nucleic Acids Res. 36, 6688–6719. https://doi.org/10.1093/nar/gkn668.

Korch, S.B., Henderson, T.A., Hill, T.M., 2003. Characterization of the hipA7 allele of *Escherichia coli* and evidence that high persistence is governed by (p)ppGpp synthesis. Mol. Microbiol. 50, 1199–1213.

Ku, S.C., Hsueh, P.R., Yang, P.C., Luh, K.T., 2000. Clinical and microbiological characteristics of bacteremia caused by *Acinetobacter lwoffii*. Eur. J. Clin. Microbiol. Infect. Dis. 19, 501–505.

Lau, C.K.Y., Krewulak, K.D., Vogel, H.J., 2016. Bacterial ferrous iron transport: the Feo system. FEMS Microbiol. Rev. 40, 273–298. https://doi.org/10.1093/femsre/fuv049.

Lean, S.S., Yeo, C.C., 2017. Small, enigmatic plasmids of the nosocomial pathogen, *Acinetobacter baumannii*: good, bad, who knows? Front. Microbiol. 8, 1547. https://doi.org/10.3389/fmicb.2017.01547.

Leplae, R., Geeraerts, D., Hallez, R., Guglielmini, J., Drèze, P., Van Melderen, L., 2011. Diversity of bacterial type II toxin-antitoxin systems: a comprehensive search and functional analysis of novel families. Nucleic Acids Res. 39, 5513–5525. https://doi.org/10.1093/nar/gkr131.

Letunic, I., Bork, P., 2019. Interactive Tree Of Life (iTOL) v4: recent updates and new developments. Nucleic Acids Res. 47, W256–W259. https://doi.org/10.1093/nar/gkz239.

Lewin, B., 2004. Transposons. In: Genes, V.I.I.I. (Ed.), Benjamin Cummings. Upper Saddle River, New Jersey, pp. 467–480.

Lewis, K., 2010. Persister cells. Annu. Rev. Microbiol. 64, 357–372. https://doi.org/10.1146/annurev.micro.112408.134306.

Ma, C.Q., Xu, P., Qiu, J.H., Zhang, Z.J., Wang, K.W., Wang, M., Zhang, Y.N., 2004. An enzymatic route to produce pyruvate from lactate. Appl. Microbiol. Biotechnol. 66, 34–39. https://doi.org/10.1007/s00253-004-1646-y.

Ma, C.Q., Xu, P., Dou, Y.M., Qu, Y.B., 2008. Highly efficient conversion of lactate to pyruvate using whole cells of *Acinetobacter* sp. Biotechnol. Prog. 19, 1672–1676. https://doi.org/10.1021/bp0341242.

Madeira, F., Park, Y. Mi, Lee, J., Buso, N., Gur, T., Madhusoodanan, N., Basutkar, P., Tivey, A.R.N., Potter, S.C., Finn, R.D., Lopez, R., 2019. The EMBL-EBI search and sequence analysis tools APIs in 2019. Nucleic Acids Res. 47, W636–W641. https://doi.org/10.1093/nar/gkz268.

Maisonneuve, E., Shakespeare, L.J., Jørgensen, M.G., Gerdes, K., 2011. Bacterial persistence by RNA endonucleases. PNAS 108, 13206–13211. https://doi.org/10.1073/pnas.1100186108.

Mateos, L.M., Ordóñez, E., Letek, M., Gil, J.A., 2006. Corynebacterium glutamicum as a model bacterium for the bioremediation of arsenic. Int. Microbiol. 9, 207–215.

Meier-Kolthoff, J.P., Göker, M., 2019. TYGS is an automated high-throughput platform for state-of-the-art genome-based taxonomy. Nature Communications 10, 1–10. https://doi.org/10.1038/s41467-019-10210-3.

Mindlin, S., Petrenko, A., Kurakov, A., Beletsky, A., Mardanov, A., Petrova, M., 2016. Resistance of permafrost and modern *Acinetobacter lwoffii* strains to heavy metals and arsenic revealed by genome analysis. Biomed. Res. Int. 2016, 3970831. https://doi.org/10.1155/2016/3970831.

Mindlin, S., Petrenko, A., Petrova, M., 2018. Chromium resistance genetic element flanked by XerC/XerD recombination sites and its distribution in environmental and clinical Acinetobacter strains. FEMS Microbiol. Lett. 365. https://doi.org/10.1093/femsle/fny047.

Mittal, S., Sharma, M., Yadav, A., Bala, K., Chaudhary, U., 2015. *Acinetobacter lwoffii* an emerging pathogen in neonatal ICU. Infect. Disord. Drug Targets 15, 184–188.

Moyed, H.S., Bertrand, K.P., 1983. hipA, a newly recognized gene of *Escherichia coli* K-12 that affects frequency of persistence after inhibition of murein synthesis. J. Bacteriol. 155, 768–775.

Overbeek, R., Olson, R., Pusch, G.D., Olsen, G.J., Davis, J.J., Disz, T., Edwards, R.A., Gerdes, S., Parrello, B., Shukla, M., Vonstein, V., Wattam, A.R., Xia, F., Stevens, R., 2014. The SEED and the Rapid Annotation of microbial genomes using Subsystems Technology (RAST). Nucleic Acids Res. 42, D206–D214. https://doi.org/10.1093/nar/gkt1226.

Pagano, M., Martins, A.F., Barth, A.L., 2016. Mobile genetic elements related to carbapenem resistance in *Acinetobacter baumannii*. Braz. J. Microbiol. 47, 785–792. https://doi.org/10.1016/j.bjm.2016.06.005.

Page, R., Peti, W., 2016. Toxin-antitoxin systems in bacterial growth arrest and persistence. Nat. Chem. Biol. 12, 208–214. https://doi.org/10.1038/nchembio.2044.

Pansegrau, W., Lanka, E., Barth, P.T., Figurski, D.H., Guiney, D.G., Haas, D., Helinski, D.R., Schwab, H., Stanisich, V.A., Thomas, C.M., 1994. Complete nucleotide sequence of Birmingham IncP alpha plasmids. Compilation and comparative analysis. J. Mol. Biol. 239, 623–663. https://doi.org/10.1006/jmbi.1994.1404.

Peleg, A.Y., Seifert, H., Paterson, D.L., 2008. Acinetobacter baumannii: emergence of a successful pathogen. Clin. Microbiol. Rev. 21, 538–582. https://doi.org/10.1128/CMR.00058-07.

Poirel, L., Nordmann, P., 2006. Genetic structures at the origin of acquisition and expression of the carbapenem-hydrolyzing oxacillinase gene blaOXA-58 in *Acinetobacter baumannii*. Antimicrob. Agents Chemother. 50, 1442–1448. https://doi.org/10.1128/AAC.50.4.1442-1448.2006.

Poirel, L., Bonnin, R.A., Nordmann, P., 2011. Genetic basis of antibiotic resistance in pathogenic *Acinetobacter* species. IUBMB Life 63, 1061–1067. https://doi.org/10.1002/iub.532.

Qamar, N., Rehman, Y., Hasnain, S., 2017. Arsenic-resistant and plant growth-promoting Firmicutes and γ-Proteobacteria species from industrially polluted irrigation water and corresponding cropland. J. Appl. Microbiol. 123, 748–758. https://doi.org/10.1111/jam.13535.

Rodriguez-R, L.M., Konstantinidis, K.T., 2014. Bypassing Cultivation To Identify Bacterial Species: Culture-independent genomic approaches identify credibly distinct clusters, avoid cultivation bias, and provide true insights into microbial species. Microbe Magazine 9, 111–118. https://doi.org/10.1128/microbe.9.111.1.

Ronneau, S., Helaine, S., 2019. Clarifying the link between toxin–antitoxin modules and bacterial persistence. J. Mol. Biol. https://doi.org/10.1016/j.jmb.2019.03.019.

Sadler, W.R., Trudinger, P.A., 1967. The inhibition of microorganisms by heavy metals. Mineral. Deposita 2. https://doi.org/10.1007/BF00201912.

Salaemae, W., Booker, G.W., Polyak, S.W., 2016. The role of biotin in bacterial physiology and virulence: a novel antibiotic target for *Mycobacterium tuberculosis*. Microbiol. Spectr. 4. https://doi.org/10.1128/microbiolspec.VMBF-0008-2015.

Salto, I.P., Tejerizo, G.T., Wibberg, D., Pühler, A., Schlüter, A., Pistorio, M., 2018. Comparative genomic analysis of Acinetobacter spp. plasmids originating from clinical settings and environmental habitats. Sci. Rep. 8, 7783. https://doi.org/10.1038/s41598-018-26180-3.

Seemann, T., 2014. Prokka: rapid prokaryotic genome annotation. Bioinformatics 30, 2068–2069. https://doi.org/10.1093/bioinformatics/btu153.

Silver, S., Phung, L.T., 2005. A bacterial view of the periodic table: genes and proteins for toxic inorganic ions. J. Ind. Microbiol. Biotechnol. 32, 587–605. https://doi.org/10.1007/s10295-005-0019-6.

Sobecky, P.A., Coombs, J.M., 2009. Horizontal gene transfer in metal and radionuclide contaminated soils. In: Gogarten, M.B., Gogarten, J.P., Olendzenski, L.C. (Eds.), Horizontal Gene Transfer: Genomes in Flux, Methods in Molecular Biology. Humana Press, Totowa, NJ, pp. 455–472. https://doi.org/10.1007/978-1-60327-853-9_26.

del Solar, G., Giraldo, R., Ruiz-Echevarría, M.J., Espinosa, M., Díaz-Orejas, R., 1998. Replication and control of circular bacterial plasmids. Microbiol. Mol. Biol. Rev. 62, 434–464.

Sullivan, M.J., Petty, N.K., Beatson, S.A., 2011. Easyfig: a genome comparison visualizer. Bioinformatics 27, 1009–1010. https://doi.org/10.1093/bioinformatics/btr039.

Thomas, C.M., Thomson, N.R., Cerdeño-Tárraga, A.M., Brown, C.J., Top, E.M., Frost, L.S., 2017. Annotation of plasmid genes. In: Plasmid, SI: ISPB Plasmid 2016. 91. pp. 61–67. https://doi.org/10.1016/j.plasmid.2017.03.006.

Tomczyk-Żak, K., Kaczanowski, S., Drewniak, Ł., Dmoch, Ł., Sklodowska, A., Zielenkiewicz, U., 2013. Bacteria diversity and arsenic mobilization in rock biofilm from an ancient gold and arsenic mine. Sci. Total Environ. 461–462, 330–340. https://doi.org/10.1016/j.scitotenv.2013.04.087.

Tomczyk-Żak, K., Szczesny, P., Gromadka, R., Zielenkiewicz, U., 2017. Taxonomic and chemical assessment of exceptionally abundant rock mine biofilm. PeerJ 5, e3635. https://doi.org/10.7717/peerj.3635.

Touchon, M., Cury, J., Yoon, E.-J., Krizova, L., Cerqueira, G.C., Murphy, C., Feldgarden, M., Wortman, J., Clermont, D., Lambert, T., Grillot-Courvalin, C., Nemec, A., Courvalin, P., Rocha, E.P.C., 2014. The genomic diversification of the whole *Acinetobacter* genus: origins, mechanisms, and consequences. Genome Biol. Evol. 6, 2866–2882. https://doi.org/10.1093/gbe/evu225.

Turton, J.F., Shah, J., Ozongwu, C., Pike, R., 2010. Incidence of *Acinetobacter* species other than a. baumannii among clinical isolates of *Acinetobacter*: evidence for emerging species. J. Clin. Microbiol. 48, 1445–1449. https://doi.org/10.1128/JCM.02467-09.

Wattam, A.R., Davis, J.J., Assaf, R., Boisvert, S., Brettin, T., Bun, C., Conrad, N., Dietrich, E.M., Disz, T., Gabbard, J.L., Gerdes, S., Henry, C.S., Kenyon, R.W., Machi, D., Mao, C., Nordberg, E.K., Olsen, G.J., Murphy-Olson, D.E., Olson, R., Overbeek, R., Parrello, B., Pusch, G.D., Shukla, M., Vonstein, V., Warren, A., Xia, F., Yoo, H., Stevens, R.L., 2017. Improvements to PATRIC, the all-bacterial bioinformatics database and analysis resource center. Nucleic Acids Res. 45, D535–D542. https://doi.org/10.1093/nar/gkw1017.

Wick, R.R., Judd, L.M., Gorrie, C.L., Holt, K.E., 2017. Unicycler: resolving bacterial genome assemblies from short and long sequencing reads. PLoS Comput. Biol. 13, e1005595. https://doi.org/10.1371/journal.pcbi.1005595.

Wilson, K., 2001. Preparation of genomic DNA from bacteria. Curr. Protoc. Mol. Biol. https://doi.org/10.1002/0471142727.mb0204s56. Chapter 2, Unit 2.4.

Xie, Y., Wei, Y., Shen, Y., Li, X., Zhou, H., Tai, C., Deng, Z., Ou, H.-Y., 2018. TADB 2.0: an updated database of bacterial type II toxin-antitoxin loci. Nucleic Acids Res. 46, D749–D753. https://doi.org/10.1093/nar/gkx1033.

Yan, G., Chen, X., Du, S., Deng, Z., Wang, L., Chen, S., 2019. Genetic mechanisms of arsenic detoxification and metabolism in bacteria. Curr. Genet. 65, 329–338. https://doi.org/10.1007/s00294-018-0894-9.

Yoon, S.-H., Ha, S.-M., Lim, J., Kwon, S., Chun, J., 2017. A large-scale evaluation of algorithms to calculate average nucleotide identity. Antonie Van Leeuwenhoek 110, 1281–1286. https://doi.org/10.1007/s10482-017-0844-4.